# The *Vitis vinifera* receptor VvLYK6 negatively regulates chitin-triggered immune responses and promotes fungal infections

Jérémy Villette[1], Tania Marzari[1], David Landry[2], Thibault Roudaire[1], Rémy Romanet[4], Agnès Klinguer[1], Nathalie Leborgne-Castel[1], Céline Vicedo[2], Virginie Gasciolli[2], Cécile Pouzet[3], Benoît Lefebvre[2], Marie-Claire Héloir[1], Benoit Poinssot[1*]

[1] Université Bourgogne Europe, Institut Agro, INRAE, UMR Agroécologie, Dijon, France

[2] Laboratory of Plant-Microbe-Environment Interactions (LIPME), Université de Toulouse, INRAE, CNRS, Castanet-Tolosan 31326, France

[3] TRI-FRAIB Imaging Platform Facilities, Fédération de Recherche Agrobiosciences Interactions et Biodiversité, Université de Toulouse, CNRS, UPS, 31320 Castanet-Tolosan, France

[4] Développement Innovation Vigne Vin Aliments Platform - UMR PAM, IUVV, Dijon, France

*****Corresponding Author: Benoit Poinssot (benoit.poinssot@u-bourgogne.fr)

ORCID

Jérémy Villette https://orcid.org/0009-0005-8772-1250

Tania Marzari https://orcid.org/0009-0006-0584-8475

David Landry https://orcid.org/0000-0002-6147-8580

Thibault Roudaire https://orcid.org/0000-0003-4780-6776

Rémy Romanet https://orcid.org/0000-0003-0779-6139

Nathalie Leborgne-Castel https://orcid.org/0000-0001-8756-4463

Virginie Gasciolli https://orcid.org/0000-0003-3240-1813

Cécile Pouzet https://orcid.org/0000-0002-2464-1940

Benoît Lefebvre https://orcid.org/0000-0002-3810-605X

Marie-Claire Héloir https://orcid.org/0000-0002-3911-3235

Benoit Poinssot https://orcid.org/0000-0001-5890-4318

## ABSTRACT

*Botrytis cinerea* is recognized as one of the most harmful fungal diseases affecting grapevine (*Vitis vinifera*), directly impacting grape yield and wine quality. Identifying new genes involved in the interaction between *V. vinifera* and *B. cinerea* appears to be the most promising strategy for enhancing grapevine resistance to this pathogen in future breeding programs. During pathogen infection, plasma membrane-localized pattern recognition receptors (PRRs) are involved in the perception of conserved microbe-associated molecular patterns (MAMPs). Among PRRs, members of the LysM receptor-like kinase family are well known to mediate recognition of fungal MAMPs to induce the plant immune signaling pathway. Interestingly, a novel member of this receptor family, named VvLYK6, was identified in grapevine as the most upregulated during a *Botrytis cinerea* infection.

Aiming to understand the role of VvLYK6 in plant immunity, we carried out an overexpression study in *Arabidopsis thaliana* and in grapevine cell suspension. The overexpression of *VvLYK6* resulted in a reduction of chitin oligomer-induced MAPKs activation, expression of defense-related genes, a reduced callose deposition and an increased plant susceptibility to three fungal pathogens. At the opposite, the CRISPR-Cas9-mediated *vvlyk6* knock-out lines generated in *V. vinifera* induce the phytoalexin-related stilbene pathway at the basal level.

Based on our findings, we concluded that VvLYK6 negatively regulates the chitin-triggered immune responses in *V. vinifera*, suggesting its potential involvement as a susceptibility gene during fungal infections.

Keywords: *Vitis vinifera*, MAMP, chitin hexamer, inhibition, plant immunity, *Erysiphe necator*, *Alternaria brassicicola*, CRISPR-Cas9.

## 1. Introduction

Grapevine (*Vitis vinifera*) is constantly subject to strong pest pressure, including viruses, insects, oomycetes such as downy mildew (*Plasmopara viticola*) and fungi with powdery mildew (*Erysiphe necator*) or grey mold (*Botrytis cinerea*). The current strategy to limit the consequences of such diseases is the use of chemicals. However, these treatments have a negative impact on the environment and human health, giving way to alternative strategies to counteract these diseases in vineyards (Pathak et al., 2022). One strategy consists in the identification of resistance (*R*) or susceptibility (*S*) genes (Qiu et al., 2015; Zaidi et al., 2018). The breeding of *R* genes in grapevine has been a key strategy in developing durable disease-resistant varieties (Xiao et al., 2023). Two members of the TIR-NB-LRR gene family from *Muscadinia rotundifolia* (a closely related species to *V. vinifera*) have been identified as major *R* genes, conferring protection against several significant grapevine pathogens (Feechan et al., 2013). Interestingly, it has been frequently observed that non-functional *S* genes also lead to resistant plants against a large panel of pathogens, making them interesting targets for breeding programs (Zaidi et al., 2018). Another strategy consists in inducing grapevine immunity by eliciting plant defenses with bioproducts (Adrian et al., 2024).

Plant innate immunity relies on two well-described defense signaling pathways (Boller and Felix 2009). The first one is the conserved microbe-associated molecular pattern (MAMP)-triggered immunity (MTI, also called PTI). The second is the effector-triggered immunity (ETI) activated after the detection of pathogen effectors by plants (Böhm et al., 2014; Zipfel 2014). MTI is the first step of plant innate immunity, with the recognition of highly conserved MAMPs released by microbes and perceived by cell-surface pattern recognition receptors (PRRs). Perception of these specific ligands by PRRs activates signal transduction into the cell. This relies on a phosphorylation cascade, involving mitogen-activated protein kinases (MAPKs), that ultimately activates transcription factors leading to the expression of defense-related genes. Depending on the MAMP's nature and concentration, appropriate defense mechanisms can be triggered such as callose deposition, production of phytoalexins (stilbenes in grapevine) or pathogenesis-related (PR) proteins (Ahuja et al., 2012; Zhou and Zhang, 2020).

Plant PRRs are diverse and include different protein families based on their extracellular domain (Ngou et al., 2022). Among PRRs, the Lysin motif receptor-like kinases (LysM-RLKs) and the Lysin motif receptor-like proteins (RLPs) are well-described to perceive different polysaccharides, including chitooligosaccharides (COS), lipochitooligosaccharides (LCO) and peptidoglycans. In every plant species, the LysM RLK family is divided in two sub-groups composed of LYK receptors with an active

kinase domain able to transduce the signal into the cell, and LYR receptors with inactive kinase domain. The LysM-RLPs (also called LYM) do nor bear kinase domain (Buendia et al., 2018).

Perception of chitin, a major component of fungal cell walls, is mediated by several LysM-RLKs/RLPs forming a functional complex at the plasma membrane to transduce the signal. Indeed, in *Arabidopsis thaliana*, the LYR AtLYK5, which has a high affinity for chitin oligomers, is known to form heterodimers with the LYR AtLYK4 (Wan et al., 2012; Cao et al., 2014; Xue et al., 2019). Despite chitin oligomers binding, AtLYK4/5 complex is unable to transmit signal due to inactive kinase domains and relies on interaction with the LYK AtCERK1 harboring a functional kinase domain while having a weak affinity for chitin oligomers (Miya et al., 2007; Cao et al., 2014). In rice, the LYK OsCERK1 is involved in both immunity and symbiosis signaling (Zhang et al., 2021). It interacts with the LYM OsCEBIP, OsLYP4, or OsLYP6 for activating immune signaling (Shimizu et al., 2010; Ao et al., 2014) or with the LYR OsMYR1 for signaling during establishment of arbuscular mycorrhiza (AM) (He et al., 2019). These different studies showed that OsCERK1 has a central role in signal transduction by its involvement in different signaling pathways. The specificity depends on the ligand and the high affinity of its cognate receptor. Indeed, a phylogenetic study showed well-conserved clades according to attributed functions (Buendia et al., 2018). For example, the LYRIII C clade, contains AtLYK5 and MtLYR4 which have a conserved function in the perception of chitin oligomers and role in MTI activation in *A. thaliana* and *Medicago truncatula*, respectively (Cao et al., 2014; Feng et al., 2019). Similarly, the LYRI A clade, including OsMYR1 and SlLYK10, have a conserved function in the perception of LCO and a role in AM establishment in rice and tomato, respectively (Buendia et al., 2016; Girardin et al., 2019; He et al., 2019; Cullimore et al., 2023).

In grapevine, recent studies support a similar model in which VvLYK1-1 and VvLYK1-2 (AtCERK1 orthologs) and VvLYK5-1 (AtLYK5 ortholog) mediate chitin signaling. Indeed, these grapevine LysM-RLKs have been shown to participate in the perception of chitin to restore MAPKs activation, defense gene expression, and pathogen resistance in the lack of function mutants of *A. thaliana* (Brulé et al., 2019; Roudaire et al., 2023). Moreover, complex formation between VvLYK1-1 and VvLYK5-1 was found to be dependent on the presence of chitin oligomers. Interestingly, in grapevine, we identified 16 LysM-RLK members divided in ten of the eleven phylogenetic clades defined in the classification of Buendia et al. (2018).

In the present study, we investigated the role of VvLYK6, a member of the *V. vinifera* LYRI B LysM-RLK clade that is poorly documented. The corresponding orthologs in various monocots and dicots, including tomato, have been described to play an important role in AM symbiosis establishment mechanisms (Li et al., 2022; Ding et al., 2024b). Interestingly, Brulé et al. (2019) showed that *VvLYK6* was the most expressed LysM-RLK during *B. cinerea* infection on susceptible mature berries. Using

functional genomic approaches, we demonstrated that VvLYK6 inhibits chitin-triggered immune responses and increases the plant susceptibility against three different fungal pathogens. Our results suggest that VvLYK6 is a receptor involved in the negative regulation of the grapevine immunity leading to the higher susceptibility to grey mold of mature berries. Thus, *VvLYK6* might be considered as a new *S* gene encoding a negative regulator of *V. vinifera* immunity.

## 2. Materials and methods

### *2.1. Plant materials and growth conditions*

*Arabidopsis thaliana* wild-type (WT) Columbia (Col-0) ecotype, *Atcerk1* mutant (GABI-Kat_096F09, allele *Atcerk1-2*; Gimenez-Ibanez et al., 2009) or transgenic lines Col-0-*p35S::VvLYK6*, Col-0-*p35S::VvLYK6-GFP*, and *Atcerk1-p35S::VvLYK6* were grown under a 10/14-h day/night cycle at 20/18°C. Transgenic lines were obtained by floral-dip transformation (Clough and Bent, 1998) of the Col-0 ecotype and *Atcerk1* mutant lines with coding sequence of *VvLYK6* (Vitvi05g00623) amplified from complementary DNA (cDNA) of the susceptible *Vitis vinifera* cv. Marselan leaves and cloned into the pFAST_R02 and pFAST_R05 (Shimada et al., 2010). Transgenic seeds were selected with glufosinate (50 mg/L) and kanamycin (50 mg/L) selection for pFAST_R02 and pFAST_R05, respectively, and subsequently genotyped (Fig. S1).

*Vitis vinifera* cv. Marselan cells were cultivated in Nitsch-Nitsch (NN) medium as detailed in Roudaire et al. (2023). For experimentations, seven-day-old cultures were diluted twice with new medium. Grapevine cells were transformed by co-cultivation with *Agrobacterium tumefaciens* culture with an absorbance of 0.3 during 2 days. Then, cells were transferred in NN medium with agar (0.7 %) supplemented with 250 mg/L cefotaxime and 50 mg/L kanamycin for selection. After 1 month, two independent lines expressing *35S-VvLYK6-GFP* were selected.

### *2.2. V. vinifera CRISPR-Cas9-generated KO lines for VvLYK6*

Grapevine cells (*V. vinifera* cv. Chardonnay) were transformed via co-cultivation with *Agrobacterium tumefaciens* harboring a plasmid construct. This construct expressed a *Zea mays* codon-optimized Cas9 (zCas9i) along with three sgRNAs designed to specifically target *VvLYK6*. WT-like (transformed but not edited) and CRISPR-Cas9-edited mutant lines for *VvLYK6* were grown under a 16/8-h day/night cycle at 26 °C. Experimental procedure to generate the two independent mutant lines for *VvLYK6* were detailed in Villette et al. (2024).

### *2.3. Analysis of VvLYK6 gene expression in developmental and pathogen-infected grapevine tissues*

Microarray and data analysis were performed as described in Kelloniemi et al. (2015) from grapevine (*Vitis vinifera* cv. Marselan) leaves and berries infected with *B. cinerea* and leaves infected by *P. viticola*. *VvLYK6* expression profile of *Vitis vinifera* cv. Garganega berries infected with or without *B. cinerea* was obtained from supplemental data of Lovato et al. (2019). Transcriptomic data highlighting differential *VvLYK6* expression profile between pre-egression and egression state in *Vitis vinifera* cv. Pinot Noir infected with *B. cinerea* were obtained from Haile et al. *(*2020).

### *2.4. Phylogenetic analysis of the VvLYKs*

Protein sequences for LysM-RLK family were retrieved using BLAST searches, in which Arabidopsis family members were used as query sequences against protein sequences from plant species detailed in Table S1. A 1000 bootstrapped phylogenetic tree gathering 96 protein sequences (Table S1) have been constructed with the Maximum Likelihood method and JTT model (Jones et al., 1992). Alignment and phylogenetic analysis were performed with MEGA X software (Kumar et al., 2018).

### *2.5. Pathogen assays*

The *B. cinerea* inoculum was produced by growing the strain BMM on solid medium (V8/2 tomato juice, 1 % agar) in the dark to promote sporulation (Zimmerli et al., 2001). Conidia were isolated and concentrated in water to infect *Arabidopsis thaliana* leaves with a final concentration of $5x10^4$ spores/mL diluted in potato dextrose broth medium (PDB, 0.6%). Four-week-old Arabidopsis leaves were cut and placed in survival conditions during *B. cinerea* infection. The *A. brassicicola* inoculum strain MIAE01824 originated from Agroecology unit collection (UMR1347, Dijon, France) was grown 20 days on solid potato dextrose agar medium (PDA, 19 $g.L^{-1}$) supplemented with sucrose (20 $g.L^{-1}$) and $CaCO_3$ (30 $g.L^{-1}$) at 20°C in the dark. Four-week-old Arabidopsis leaves were cut and placed in survival conditions during *A. brassicicola* infection. Lesion surfaces caused by these two necrotrophic fungi were measured with imageJ software (https://imagej.net/ij/).

*Erysiphe necator* assays were performed as described by Roudaire et al. (2023). Fungal structures were visualized using a Leica DMA light microscope (magnification x400). For each treatment, 100 germinated spores were evaluated. The percentage of successful epidermal cell penetration was determined based on the presence of a haustorium within the cell or the emergence of secondary

hyphae from the appressorium, as previously described by Roudaire et al. (2023). Three biological independent experiments were performed.

### *2.6. Confocal microscopy*

Confocal microscopy was performed using a Leica TCS SP8 multiphoton microscope with a 40X oil-immersion objective. Marselan suspension cells and leaf segments of *A. thaliana* lines expressing *VvLYK6* tagged with GFP were mounted directly or in ultrapure water between slide and coverslips, respectively and observed. For plasma membrane staining, samples were incubated in 10 µM FM4-64 during 10 min prior to observation. Fluorescent markers were excited with the 488 nm laser. GFP and FM4-64 emissions were bandpass filtered at 500-525 nm and between 616 - 694 nm, respectively. Pictures were then treated with LAS X software.

### *2.7. Elicitors and plant treatment*

In this study, we used as elicitors a purified hexamer (DP6) of chitin (GLU436, Elicityl, Crolles, France at a concentration of 0.05 g/L) and flg22 peptide from *X. campestris* pv. campestris strain 305 (QRLSSGLRINSAKDDAAGLAIS) at $10^{-6}$ or $10^{-8}$ M, depending on the bioassay (Trdá et al., 2014). For *A. thaliana* treatments, four-weeks old plant leaves were pre-infiltrated with ultrapure water and placed on 6-wells plate containing ultrapure water during 4 hours. Then, ultrapure water was replaced by either ultrapure water (control) or elicitors in contact with leaves during 10 min for MAPKs activation and one hour for RT-qPCR experiments before freezing samples in liquid nitrogen.

Grapevine cell suspensions were equilibrated at 0.1 g/mL and shacked under the same conditions as for their culture. Treatment was done in a volume of 20 mL with a final concentration of 0.05 g/L chitin DP6, cells were harvested in liquid nitrogen at 10 min post-treatment for MAPKs activation and 1hour post-treatment for RT-qPCR analysis.

### *2.8. MAPKs phosphorylation and real-time quantitative PCR (RT-qPCR) analysis*

For MAPK phosphorylation, treated *A. thaliana* leaves or grapevine cells were crushed in liquid nitrogen and total proteins were extracted with a solution containing 50mM HEPES (pH 7.5), 5mM EGTA (pH 8.1), 5 mM EDTA, 1mM $Na_3VO_4$, 50 mM β-glycerophosphate, 10 mM NaF, 1 mM de phenylmethanesulfonyl fluoride, 5 mM dithiothreitol and complete EDTA-free protease inhibitor cocktail (Roche). Phosphorylation of MAPKs was detected by immunoblotting of 25µg total proteins using an anti-p42/44-phospho-ERK antibody (Cell Signaling Technology). Antibody was then revealed using ECL prime (Cytiva) western blotting detection reagent with an Amersham

ImageQuant800 (Cytiva). Quantification of MAPKs intensity was normalized by total proteins stained by Ponceau red with the ImageQuant software.

For RT-qPCR experiments, treated leaves or cells were crushed in liquid nitrogen and total RNA was extracted with the SV Total RNA Isolation System with DNAse treatment (Promega). First-strand cDNAs were synthesized with the High-Capacity cDNA Reverse Transcription kit (Applied Biosystems). RT-qPCR was performed in a ViiA™ 7 Real-Time PCR system (Applied Biosystems) with 10 ng cDNA and 1X GoTaq® qPCR Master Mix (Promega). Relative gene expression was assessed taking into consideration the efficiency (E) of each reaction calculated by the LinRegPCR quantitative PCR data analysis program (Ruijter et al., 2009). Gene expression values were normalized with two housekeeping genes corresponding to *AtRHIP1* (At4g26410) and *AtPTB1* (At3g01150) for RT-qPCR experiments on *A. thaliana*, *VvRPL18B* (Vitvi05g00033) and *VvVPS54* (Vitvi10g01135) for RT-qPCR assays on grapevine cells (*Vitis vinifera* cv. Marselan) and *VvEF1α* (Terrier et al., 2005) and *VvVATP16* (Gamm et al., 2011) on CRISPR-Cas9-generated grapevine lines (*Vitis vinifera* cv. Chardonnay). All primers used are listed in Table S2.

### *2.9. Callose deposition analysis*

Four-week-old Arabidopsis were sprayed on both sides with either water (as control) or chitin DP6 (0.05 g/L). Four days post-treatment, two leaves of three independent plants per condition were sampled and fixed in absolute ethanol during one night. The aniline blue staining was performed as detailed in Roudaire et al. (2023). Leaves were then observed on adaxial side by epifluorescence microscopy under λex = 340-380 nm and λem = 425 nm, magnification x100, Leica DMRB. Callose deposits were acquired for each condition using the Nis Elements BR software (Nikon) with the DS-5Mc-U1 digital photomicrographic camera (Nikon). Image analysis was then performed on the Fiji application as described in Mason et al. (2020) with Trainable Weka Segmentation plugin.

### *2.10. Transient expression and FRET-FLIM analysis and co-immunopurification*

The transient expression in *Nicotiana benthamiana* leaves were previously described in Girardin et al. (2019) using Agrobacteria containing a cassette overexpressing either VvLYK1-1$^{G328E}$ (Brulé et al., 2019) fused with a C-terminal Cyan Fluorescent Protein (CFP) alone or with VvLYK6 or VvLYK5-1 (Roudaire et al., 2023) tagged with a C-terminal Yellow Fluorescent Protein (YFP) (Karimi et al., 2005). The kinase-dead mutant version of VvLYK1-1 (VvLYK1-1$^{G328E}$) was generated using the Quik Change Site-Directed Mutagenesis protocol (Liu and Naismith, 2008). FLIM was performed on an inverted LEICA DMi8 microscope equipped with a TCSPC system from PicoQuant. The excitation of the CFP donor at 440 nm was carried out by a picosecond pulsed diode laser at a repetition rate of 40

MHz, through an oil immersion objective (63×, N.A. 1.4). The emitted light was detected by a Leica HyD detector in the 450-500 nm emission range. Images were acquired with acquisition photons of up to 1500 per pixel. Data were acquired in 3 independent experiments and pooled. From the fluorescence intensity images, the decay curves of CFP were calculated per pixel and fitted (by Poissonian maximum likelihood estimation) with either a double- or tri-exponential decay model using the SymphoTime 64 software (PicoQuant, Germany). The double-exponential model function was applied for donor samples with only CFP present. The tri-exponential model function was used for samples containing CFP and YFP. For co-immunopurification, the sequence coding VvLYK1-1$^{G328E}$ was fused to the sequence coding a triple hemaglutin (HA) tag. VvLYK1-1$^{G328E}$:HA and VvLYK6:YFP or VvLYK5-1:YFP were expressed into *N. benthamiana*. Leaf material was collected 3 days after infiltration and co-immunopurification was performed as described in Ding et al. 2024a, except that anti-HA beads (pierce Anti-HA magnetic beads, 88836) were used for purification and anti-HA-HRP antibodies (Roche, Anti-HA-Peroxidase High affinity from rat IgG1, 12013819001) were used for Western-blotting. CO6 at 0.1 g/L was infiltrated into leaves before harvest and added in the IP buffer for protein solubilisation and wash of the beads.

### *2.11. Microsomal fraction preparation and binding assay*

Preparation of microsomal fraction, and binding assays were previously described in Girardin et al., 2019. CO5-biotin and CO7-biotin were synthesized as detailed in Cullimore et al., 2023. Briefly, binding assays with CO5-biotin and CO7-biotin were conducted on microsomal fractions in binding buffer described in Girardin et al. (2019) for 1h at 4 °C. For western-blotting, proteins were separated by SDS-PAGE using homemade 6 % polyacrylamide gels and transferred onto a nitrocellulose membrane with a transblot system (Bio-rad). The membranes were blocked for 1h and incubated for 1h with the following antibodies: αGFP (11814460001, Roche, 1:3000), and then goat αMouse-HRP (1706516, Bio-Rad, 1:10000) or streptavidin-HRP (S911, Invitrogen, 1:3000). The chemiluminescent signal from HRP was observed using Chemidoc system (Bio-Rad).

### *2.12. Liquid chromatography-mass spectrometry (LC-MS) analysis*

The samples were analyzed using ultra high-pressure liquid chromatography (UHPLC) (Dionex Ultimate 3000, ThermoFisher, Waltham, MA, USA) coupled to a MaXis plus MQ ESI-Q-ToF mass spectrometer (MS) (Bruker, Bremen, Germany) in positive ionization mode, as describe in Puyo et al., 2024. For the pre-treatment of masses, Burker Compass MetaboScape Software (v. 8.0.1, Bruker, Mannheim, Germany) was used. The masses extracted were those with an intensity higher than the threshold of 1000 and which were found in at least 20% of the samples, with 40% for recursive

parameters. Annotation of the features have been realized using MassBank database. Resveratrol has been annotated with level 2 according to Schymanski et al. (2014).

## 3. Results

### *3.1. Analysis of VvLYK6 gene expression suggests an important role during B. cinerea infection.*

To investigate the role of *VvLYK6* in grapevine immunity, we analyzed its expression profile from our previous transcriptomic dataset (Kelloniemi et al., 2015). Our data showed that *VvLYK6* is up-regulated in susceptible *V. vinifera* leaves after 24 and 48h of *B. cinerea* infection while its expression does not change when leaves are infected with *P. viticola* (Fig. 1A). Given that VvLYK6 belongs to the LysM-RLK family known to perceive COS, these results are consistent with the presence of chitin in the fungal cell wall of *B. cinerea*, which is nearly absent in that of the oomycete *P. viticola*. However, *VvLYK6* expression was not significantly induced in grapevine cells treated with chitin hexamers (Fig. S2A). We also observed that *VvLYK6* expression is induced after 48h of *B. cinerea* infection on grapevine fruits (Fig. 1B) and particularly in infected mature berries (Fig. 1C) which are known to be very susceptible to grey mold (Kelloniemi et al., 2015). To corroborate these results and confirm the upregulation of *VvLYK6* during *B. cinerea* infection, we analyzed other publicly available transcriptomic data (Fig. S2B-C). In a first study on mature berries of the susceptible *Vitis vinifera* cv. Garganega inoculated or not with *B. cinerea*, *VvLYK6* expression was significantly increased in infected berries compared to uninfected ones twelve days post-inoculation (Lovato et al., 2019, Fig. S2B). In a second study comparing ripe berries of the susceptible *V. vinifera* cv. Pinot Noir with and without visible symptoms of *B. cinerea* infection (referred to as egression and pre-egression, respectively), the expression of *VvLYK6* was significantly upregulated only in berries displaying visible symptoms (Haile et al., 2020, Fig. S2C). Taken together, these results showed a correlation between *VvLYK6* upregulation in mature grapevine berries and their high susceptibility to *B. cinerea*.

### *3.2. VvLYK6 belongs to the LYRI B clade with conserved domain of LysM-receptor like kinase.*

To investigate the function of VvLYK6, we firstly performed a phylogenetic analysis including several plant species which possess well-described LysM-RLKs involved in different functions (immunity and/or symbiosis). We retrieved LysM-RLK proteins from *A. thaliana*, *Hordeum vulgare*, *Oryza sativa*, *Medicago truncatula*, *Musa acuminata*, *Prunus persica*, *Solanum lycopersicum* and *Vitis*

*vinifera* (Supplementary Table S1). Ninety-six protein sequences have been selected to perform a maximum-likelihood phylogenetic tree (Fig. 2A). Phylogenetic tree exhibits the well-known two sub-groups (LYKs and LYRs) sub-divided in eleven clades described by Buendia et al. (2018). The 16 members of the LysM-RLK family in *Vitis vinifera* are distributed across all clades, except for the LYKIV clade, which is not conserved among all dicots (Fig. 2A). We focused our study on VvLYK6 (black arrow), belonging to the LYRI B clade, which function has never been characterized in *Vitis vinifera*. We first analyzed the putative structure of VvLYK6 and confirmed that all LysM-RLK conserved domains were retrieved in VvLYK6: a signal peptide, three extracellular LysM domains, a transmembrane domain, and a cytoplasmic putative serine/threonine kinase domain (Fig. 2B, Table S3). Concerning the intracellular kinase domain analysis, most of all amino acid motifs known to be important for the kinase activity of the LYKI members (AtCERK1, VvLYK1-1, VvLYK1-2) were aligned with the LYRI B orthologs, including VvLYK6 (Fig. 2B). However, the deletions observed in the glycine rich loop and the lack of conservation in the catalytic loop and the activation segment involved in kinase activity suggests a kinase domain putatively deprived of kinase activity for VvLYK6 and all members of the LYRI B clade (Hanks et al., 1988; Klaus-Heisen et al., 2011). Indeed, the glycine-rich loop is composed of three to four conserved glycine residues for most of the members of the LYK sub-group having kinase activity, whereas only one glycine residue is present for the LYRI B sub-group. Then, other known motifs well conserved in the LYK sub-group with an active kinase domain such as the catalytic loop (RD) and the activation segment (DFG) are not conserved in the LYRI B clade (Fig. 2B). So far, all members of the LysM-RLK family have been described as localized at the plasma membrane (Buendia et al., 2018). We checked the sub-cellular localization of VvLYK6 in *Arabidopsis thaliana* and *Vitis vinifera* by expressing a GFP-tagged version of VvLYK6 in C-terminal. Selected transgenic lines showed a green fluorescence of VvLYK6-GFP co-localizing with the red fluorescence of the plasma membrane marker probe FM4-64 (Brandizzi et al., 2004) in the two-plant species (Fig. 2C, Fig. S3). Plasmolysis experiments confirmed that VvLYK6 followed the plasma membrane shrinking (Fig. 2C). Both observations are consistent with VvLYK6 being localized at the plasma membrane.

### *3.3. Constitutive expression of VvLYK6 in A. thaliana increases its susceptibility to B. cinerea and other adapted or non-adapted fungal pathogens.*

To study the role of *VvLYK6* during *B. cinerea* infection, and taking advantage that *VvLYK6* does not possess ortholog in *A. thaliana*, we constitutively expressed *VvLYK6* from the susceptible *V. vinifera* cv. Marselan under the control of the constitutive *CaMV35S* promoter (*p35S*) in the WT ecotype Col-

0 of *A. thaliana*. Three independent lines expressing *VvLYK6* with a high transcript level were selected (Fig. S4A). To investigate the role of *VvLYK6* during fungal infections, leaves were first infected with *B. cinerea* and lesion areas were quantified at 3 days post-inoculation (dpi). Fig. 3A and Fig. S4B show a significant increase in susceptibility to *B. cinerea* (of around 50%) for the three independent lines overexpressing *VvLYK6* when compared to WT plants. We then investigated the influence of *VvLYK6* expression for other pathogenic fungi. First, we chose another necrotrophic fungus *Alternaria brassicicola* that is adapted to Brassicaceae. At 5 dpi with *A. brassicicola*, the three lines constitutively expressing *VvLYK6* showed an average lesion area significantly increased between 26% and 67% in comparison to the WT infected plants referred as 100% (Fig. 3B, Fig. S4C). Finally, using the non-adapted biotrophic fungus *Erysiphe necator* (grapevine powdery mildew), the three lines constitutively expressing *VvLYK6* also exhibited a significantly increased penetration in epidermal cells when compared to WT plants, with around 50% and 30% of penetrated cells, respectively (Fig. 3C). Our results suggest that VvLYK6 might inhibit plant immune responses to promote fungal spreading.

### *3.4. Constitutive expression of VvLYK6 inhibits chitin-triggered immune responses in A. thaliana.*

To decipher the function of VvLYK6, we studied the early defense events induced by chitin through analyzing the MAPKs phosphorylation level. As previously reported (Roudaire et al., 2023), chitin oligomers trigger in Arabidopsis WT plants the transient phosphorylation of two MAPKs of 43 and 47 kDa (Fig. 4A), which were previously identified as MPK3 and MPK6, respectively (Claverie et al., 2018). Interestingly, both MAPKs phosphorylation induced 10 min after chitin hexamer (DP6) treatment was significantly reduced by around 40% in the three independent VvLYK6-expressing lines in comparison to WT (Fig. 4A-B). A putative delayed phosphorylation of the MAPKs was checked 20 min after treatment to rule out a shift in MAPKs activation in transgenic lines (Fig. 4A). Moreover, the expression of two defense genes encoding flagellin-induced receptor kinase 1 (*AtFRK1*) and respiratory burst oxidase homologue D (*AtRBOHD*), known to be induced by chitin DP6 treatment (Morales et al., 2016, Brulé et al., 2019), was also significantly reduced (Fig. 4C-D). Indeed, the level of *AtFRK1* expression following chitin DP6 treatment was reduced between 56 and 71% in the three independent *VvLYK6*-expressing lines (Fig. 4C). Secondly, the normalized transcript level of *AtRBOHD* was reduced between 67% and 74% in the three independent *VvLYK6*-expressing lines (Fig. 4D). Additional immune-related genes linked to various hormonal signaling pathways, such as salicylic acid (SA) and jasmonate (JA), were analyzed (Spoel et al., 2003). No significant differences in the expression of the SA- and JA-associated genes *PR1* and *PDF1.2* were detected between the

three independent VvLYK6-expressing lines and the WT following chitin DP6 treatment (Fig. S5). To further explore the function of VvLYK6, we analyzed the effect of its constitutive expression on callose deposition, a later defense event. As shown in many studies, chitin is well known to induce callose deposition in *A. thaliana* leaves (Roudaire et al., 2023). Compared to the WT, all transgenic lines expressing VvLYK6 showed a significantly lower percentage of callose deposits 4 days after chitin DP6 treatment (Fig. 4E-F). After chitin DP6 treatment, 0.2 % of the WT total leaves area showed callose deposits whereas the three transgenic lines showed a mean area of callose deposits of 0.04 %, almost similar to water treatment (Fig. 4E-F). Taken together, these results clearly indicate that the expression of *VvLYK6* in *A. thaliana* inhibits the chitin-triggered immunity.

We focused our study on the role of VvLYK6 during fungal infections or after chitin treatment because we found that *VvLYK6* is induced during *B. cinerea* infection. However, to test the specificity of VvLYK6 for chitin oligomers versus other elicitors, we measured the responses to a bacterial MAMP: the flagellin-derived peptide flg22 (Trdá et al., 2014). The MAPKs phosphorylation was compared after elicitation by flg22 in the WT and the three *VvLYK6*-expressing lines. The immunoblotting of MAPKs phosphorylation indicates that no difference could be observed 10 min after flg22 treatment (Fig. S6A). As flg22 is also known to inhibit plant growth in *A. thaliana* (Vetter et al., 2012), seedlings growth inhibition assays were also performed with flg22. The three independent lines expressing *VvLYK6* did not show any significant difference in growth inhibition compared to WT plants after 12 days on 1 µM flg22 (Fig. S6B). These results demonstrate that *VvLYK6* expression in *A. thaliana* does not affect flg22-triggered immune signaling pathway but seems to be specifically involved in chitin-activated immune responses related to fungal pathogens.

### *3.5. VvLYK6 represses chitin-triggered immunity in grapevine (Vitis vinifera).*

To validate the findings observed in *A. thaliana*, we investigated the function of VvLYK6 in *V. vinifera*. We selected two independent grapevine cell lines constitutively expressing VvLYK6 tagged with GFP and exhibiting high levels of transcripts and proteins (Fig. S7A-B). Chitin oligomers were shown to elicit the phosphorylation of two MAPKs (at 45 and 49 kDa, respectively) in grapevine (Brulé et al., 2019). Interestingly, the chitin DP6-induced MAPKs phosphorylation was statistically significantly reduced by 25% to 35% for both MAPKs after a 10-min treatment in the two transgenic lines over-expressing VvLYK6 OE#1 and OE#2, respectively (Fig. 5A, S7C). In addition, the relative expression of two defense genes linked to the *V. vinifera* stilbene pathway for the production of phytoalexins, encoding the phenylalanine ammonia lyase (*VvPAL*) and stilbene synthase (*VvSTS1.2*),

were quantified 1 h after chitin DP6 treatment (Fig. 5B-C). The constitutive expression of *VvLYK6* significantly affect the induction of *VvPAL* and *VvSTS1.2* following the chitin DP6 treatment. Indeed, the well-described up-regulation of these two-defense genes were significantly reduced by more than 50% in the two transgenic cell lines 1 h after DP6 treatment in comparison to WT cells (Fig. 5B-C). Taken together, these data suggest that VvLYK6 is also a negative regulator of chitin-triggered immune responses in *V. vinifera*.

### *3.6. VvLYK6 forms a receptor complex with VvLYK1-1 in presence of chitin oligomers*

During a fungal infection or in presence of chitin, VvLYK1-1 has been described to be the co-receptor playing a critical role in the chitin-triggered immune signaling (Brulé et al., 2019). Interestingly, only VvLYK1-1 has also been shown to form a complex with VvLYK5-1 to perceive chitin and activate the defense signaling pathways (Roudaire et al., 2023). To repress MTI when VvLYK6 is overexpressed, we can postulate a potential interaction between the grapevine functional co-receptor VvLYK1-1 and VvLYK6. For that, we performed FRET-FLIM experiments after transient expression of both genes fused to either CFP and YFP, respectively. As the constitutive expression of VvLYK1-1 induced a strong cell-death when expressed in *Nicotiana benthamiana*, we used a dead-kinase version of VvLYK1-1 with the G328E mutation (VvLYK1-1$^{G328E}$-CFP). As expected, the CFP lifetime in VvLYK1-1$^{G328E}$-CFP expressed alone is not influenced by chitin (Fig. 6A). During VvLYK1-1$^{G328E}$-CFP and VvLYK6-YFP co-expression, the addition of chitin DP6 resulted in a significant decrease of CFP lifetime, indicating an *in vivo* ligand-dependent interaction between these two LysM-RLKs (Fig. 6A). Additional co-immunoprecipitation (Co-IP) assays confirmed the interaction between VvLYK6-YFP and VvLYK1-1$^{G328E}$-HA in presence of chitin DP6 (Fig. 6B). For both experiments, VvLYK5-1 was used as a positive control as it was previously described to interact with VvLYK1-1 in a ligand-dependent manner (Fig. 6A-B, Roudaire et al., 2023). It is interesting to note that VvLYK6 and VvLYK1-1 mainly interact in presence of chitin DP6 suggesting that VvLYK6 might have affinity for chitin oligomers. Indeed, it is known that LYRI B orthologs have a high affinity for short- and long-chain chitin oligomers (Li et al., 2022; Ding et al., 2024b). Consequently, we employed cross-linkable biotinylated versions of CO5 (CO5-biotin) and CO7 (CO7-biotin) to evaluate the binding affinity of VvLYK6-YFP to chitin oligomers. Surprisingly, in contrast to its orthologs in *Brachypodium distachyon* (BdLYR2) or in *Medicago truncatula* (MtLYR8), VvLYK6 does not bind chitin oligomers (CO5 or CO7) with high affinity (Fig. 6C, Li et al., 2022; Ding et al., 2024b). We cannot exclude that in contrast to BdLYR2, VvLYK6 might be not correctly folded when overexpressed in *N. benthamiana* leaves, resulting in a nonfunctional protein, or that VvLYK6 needs to be associated with VvLYK1-1 to properly bind chitin oligomers and perform the signal transduction. In agreement with these results,

the constitutive expression of *VvLYK6* in the Arabidopsis loss-of-function mutant *Atcerk1* cannot activate MAPKs phosphorylation and induce *FRK1* expression after chitin DP6 treatment (Fig. S8).

### *3.7. VvLYK6 has a role in basal grapevine immunity*

To further explore the VvLYK6 function in grapevine immunity, we generated knock-out (KO) lines in *V. vinifera* using CRISPR-Cas9 technology. Two *Vvlyk6* mutants, designated KO#1- and KO#2-*vvlyk6*, were selected. These mutants exhibited two distinct types of mutations, each leading to different truncated predicted proteins (Fig. 7A-B). We then focused on the stilbene-related pathway as this pathway was shown to be down-regulated in *VvLYK6*-overexpressing lines (Fig. 5B-C). First, we examined the expression of grapevine defense genes associated with the stilbene pathway (*VvSTS1.2)* in the two independent KO-*Vvlyk6* lines. Interestingly, *VvSTS1.2* expression showed a significant increase in the two KO-lines, being three to four times higher than in the WT-like one at basal state (Fig. 7C). To corroborate these findings, LC-MS analysis indicated a higher resveratrol content (the major stilbene phytoalexin) in both mutant lines (KO#1 & KO#2) compared to the unmutated transgenic WT-like line (Fig. 7D). In contrast, no significant differences in the expression of SA- and JA-associated genes were detected between the two mutant lines compared to the WT-like one (Fig. S9). These results further emphasize the important role of VvLYK6 in specific grapevine immune responses, even at basal state.

## 4. Discussion

*B. cinerea* is one of the most devastating fungi for many plant species. This necrotrophic fungus is well-known to mainly infect susceptible *V. vinifera* mature berries, decreasing yield and quality of the must during wine making (Fillinger and Elad, 2016). Numerous transcriptomic studies have revealed upregulation of specific genes during berry ripening, a stage known to be highly susceptible to infection (Kelloniemi et al., 2015; Lovato et al., 2019; Haile et al., 2020). In addition, chitin, which is among the major structural components of fungal cell walls, is considered as a MAMP. Consequently, in the context of *B. cinerea* infection, we focused on the well-described family of LysM-RLKs, known to be involved in the perception of chitin oligomers and the establishment of immunity. In susceptible *V. vinifera* varieties, *VvLYK6* has been shown to be the most highly expressed LysM-RLK during *B. cinerea* infection in mature berries (Kelloniemi et al., 2015; Brulé et al., 2019) and these data are supported by additional transcriptomic analyses (Lovato et al., 2019; Haile et al., 2020). Our study sheds light on the role of the new LYRI B member VvLYK6 during *B. cinerea* infection and in

presence of chitin oligomers. Surprisingly, we found that VvLYK6 from a susceptible *V. vinifera* variety does not contribute to grapevine immunity but rather inhibits plant defenses during *B. cinerea* infection. Indeed, the constitutive expression of *VvLYK6* in *A. thaliana* significantly increases the plant susceptibility to *B. cinerea*. More accurately, we showed that the inhibitory function of VvLYK6 is only involved in chitin-triggered defense pathway related to fungal pathogens.

In *V. vinifera*, the constitutive expression of *VvLYK6* have a similar effect on the inhibition of chitin-triggered pathway. Related to these results, VvLYK6 can form a heterodimer complex with VvLYK1-1 in presence of chitin oligomers, leaving way to potential competition between VvLYK6 and VvLYK5-1 to form a complex with VvLYK1-1 (Roudaire et al., 2023). When *VvLYK6* is upregulated during *B. cinerea* infection in mature berries, a high proportion of complexes between VvLYK1-1 and VvLYK6 could be formed considering that *VvLYK6* upregulation does not impact the *VvLYK5-1* expression (Fig. S7D). This may negatively control the complex formation between VvLYK1-1 and VvLYK5-1 leading to a proposed model in which the expression level of *VvLYK6* modulates chitin-triggered immunity in grapevine (Fig. 8). With regard to the LysM-RLK family, a similar model has been described in rice. Indeed, the well-described rice ortholog of VvLYK1-1, OsCERK1, is known to be involved both in immunity, by interacting with OsCEBIP, and in AM, by interacting with OsMYR1. When OsMYR1, belonging to LYRI A clade, is constitutively expressed in rice, plant resistance decreases significantly (Zhang et al., 2021). In another family of RLK, a Leucine-Rich Repeat (LRR)-RLK named BIR2 acts as a negative regulator by forming a complex with BAK1 to control the complex formation of BAK1 with other specific ligand-binding receptors such as FLS2 in presence of MAMPs (Halter et al., 2014).

During chitin-triggered immunity in *V. vinifera*, VvLYK6 appears to be negatively correlated with the expression of the well-established defense-related gene *VvPAL* and *VvSTS1.2*, encoding the phenylalanine ammonia lyase and the stilbene synthase, respectively. These two enzymes catalyze the last step of the resveratrol production, the main grapevine phytoalexin. When VvLYK6 is overexpressed in grapevine cells, *VvPAL* and *VvSTS1.2* expression is significantly suppressed. These findings align closely with the *V. vinifera* susceptibility to *B. cinerea* during berry ripening. Indeed, green berries typically exhibit a basal resistance to *B. cinerea* whereas mature berries become very susceptible at the harvest. At the veraison stage, Kelloniemi et al. (2015) showed that the defense-related gene *VvPAL* and *VvSTS1.2* are significantly upregulated in berries infected by *B. cinerea*, leading to the accumulation of resveratrol, while the expression of *VvLYK6* remains very low. Conversely, in mature berries, the upregulation of *VvLYK6* is accompanied by a non-induction of the defense-related genes *VvPAL* and *VvSTS1.2*, resulting in increased susceptibility to this pathogen (Kelloniemi et al., 2015). Our findings highlight the important role of VvLYK6 as a key molecular

component associated with the expression of *VvPAL* and *VvSTS1.2*, thus influencing the grapevine susceptibility during *B. cinerea* infection. It's worth noting that in another species, such as tomato, ripe fruits are considerably more vulnerable to *B. cinerea* compared to unripe fruits (Silva et al., 2021). In this study, the authors conducted transcriptomic analyses which unveiled an upregulation of the tomato *VvLYK6* ortholog, identified as *SlLYK9* (Fig. 1), in ripe fruits infected by necrotrophic fungi *B. cinerea* and *Rhizopus stolonifera* (Fig. S10). As for *VvLYK6* in grapevine, the upregulation of *SlLYK9* correlates with the susceptibility of mature fruits in tomato suggesting a similar role in plant defense inhibition (Silva et al., 2021). Consequently, a new function could be attributed to the LysM RLKs belonging to the LYRI B clade. Until now, LYRI B members were primarily associated with functions in symbiosis establishment (Li et al., 2022; Ding et al., 2024b), but it appears that members of this clade can play a larger role as negative regulators of the plant immunity in diverse organs of different plant-fungal interactions. This is consistent with their expression in both roots and aboveground tissues (leaves and fruits) in grapevine and tomato (Fig. S11). Such a dual function was also found for other LysM-RLKs. Genes in the LYRI A clade are involved in the establishment of symbiosis and could be positive or negative immune regulators, depending on the plant species (Buendia et al., 2018, Zhang et al., 2021), but their expression is restricted to roots. Similarly, LYRIII C-genes are negative regulators for both immunity and AM establishment (Wang et al., 2023), and are expressed both in roots and in aboveground tissues. LYRI B-genes may therefore act as repressors of plant immunity in the aerial parts during *B. cinerea* infection while also contributing to AM establishment in roots. A role for *VvLYK6* in the establishment of AM should be investigated because, unlike other LYRI B proteins, it does not appear to have conserved its high affinity for COS.

From an evolutionary perspective, we analyzed the LYK6 receptor from *Muscadinia rotundifolia* (MrLYK6), a species naturally resistant to *Botrytis cinerea* and closely related to *Vitis vinifera* (Gabler et al., 2003). Alignment of the two LYK6 protein sequences from *M. rotundifolia* and *Vitis vinifera* shows a sequence identity of 95.4% with over half of the variations identified in the LysM2 domain (Fig. S12A). This domain has been characterized to play a critical role in chitin binding in OsCEBIP, AtCERK1 and OsCERK1 with specific residues directly involved in this binding (Liu et al.; 2012; Hayafune et al., 2014; Xu et al., 2023). Interestingly, multiple alignment revealed variations between VvLYK6 and MrLYK6 sequences in amino acids found to be critical for chitin binding in OsCEBIP, AtCERK1 and OsCERK1 (Fig. S12A-B). Moreover, we used alphafold-3 to compare the predicted three-dimensional structure of the LysM2 domain of VvLYK6 and MrLYK6 (Fig. S12C), based on the crystallized structure of OsCERK1 bound to a chitin hexamer (Xu et al., 2023). These structural predictions reveal differences in both charges and conformations within the chitin-binding region between the LysM2 domains of VvLYK6 and MrLYK6. Taken together, these natural variations

identified in the LysM2 domain of VvLYK6 may explain its undetectable affinity for chitin oligomers when expressed alone (Fig. 6C). Conversely, putative chitin binding of MrLYK6 might contribute to greater resistance of *M. rotundifolia* to *B. cinerea*.

## 5. Conclusions

To conclude, our study indicates that VvLYK6 forms a chitin-induced receptor complex with VvLYK1-1 and that its overexpression negatively regulates plant immune responses and enhances susceptibility to *B. cinerea* and other fungal pathogens. These findings suggest that VvLYK6, particularly in susceptible grapevine cultivars of *V. vinifera*, functions as a susceptibility (*S*) gene. Targeted knock-out of *VvLYK6* therefore represents a compelling strategy for improving grapevine resistance to *B. cinerea* and other fungal pathogens. In line with the growing interest in *S* genes as complementary or alternative targets to classical resistance (*R*) genes in crop breeding (Zaidi et al., 2018), *VvLYK6* emerges as a promising candidate for genome editing approaches. Moreover, we identified naturally occurring mutations between *LYK6* from *Muscadinia rotundifolia* and *Vitis vinifera*, which could underlie differences in disease resistance. These naturally beneficial *VvLYK6* variants could be harnessed through base editing technologies to precisely engineer enhanced resistance traits, offering a novel and sustainable avenue for grapevine breeding.

ACKNOWLEDGEMENTS

We acknowledge Abdelwahad Echairi and Anna Beslic (SATT Sayens, Dijon, France) for the *E. necator* strain. We also acknowledge Dr Christian Steinberg for the *A. brassicicola* inoculum strain MIAE01824 originated from Agroecology unit collection (UMR1347, Dijon, France). We acknowledge Cécile Blanchard for her technical support concerning the infection with the different pathogens. We acknowledge Régis Gougeon for accessibility to DIVVA platform and collaboration and Elodie Noirot for confocal microscopy supports from the regional Centre of Microscopy/DImaCell platform (Dijon, France). We also acknowledge France-BioImaging infrastructure supported by the French National Research Agency (ANR-10-INBS-04).

FUNDING SOURCES

This work has been supported by Plant2Pro® Carnot Institute in the frame of its 2020 call for projects (VitiLYKs project, grant #C4520) which is supported by the French National Research Agency (ANR 20-CARN-024-01) and the PPR VITAE (ANR 20-PCPA-0010).

## COMPETING INTERESTS

The authors declare no potential conflict of interest.

## AUTHOR CONTRIBUTIONS

JV performed the most of experiments and data analysis. JV, BL, MCH and BP designed the project, experiments and wrote the article. JV produced all transgenic lines of *A. thaliana* excepts lines expressing *VvLYK6* in Col-0 genetic background generated by TR. JV performed all experiments carried out on *A. thaliana* described in this article. NLC and AK transformed and selected grapevine cells for *VvLYK6* overexpression. TM performed all experiments on grapevine cells including treatments and RT-qPCR, Western Blot were done by JV. DL performed transient expression of *VvLYK* in tobacco, microsomal fractions, binding assays and FLIM experiments with CP. TM, CV and VG performed co-IP experiment. RR performed LC-MS experiments and associated analysis. All authors contributed to the article and approved the submitted version.

## DATA AVAILABILITY

All data supporting the findings of this study are available within the paper and its supporting information are published online, and the materials of this study are available from the corresponding author upon reasonable request.

## FIGURE LEGENDS

**Fig. 1.** *VvLYK6* is induced during *Botrytis cinerea* infection on grapevine leaves and mature berries. **(A)** *VvLYK6* expression profiles analyzed at 0, 24 and 48 h post-inoculation on leaves infected either by *Botrytis cinerea* or *Plasmopara viticola*. **(B)** *VvLYK6* expression profiles analyzed at 0, 24 and 48 h post-inoculation on ripe berries infected or not with *B. cinerea*. **(C)** Comparison of *VvLYK6* expression on grapevine berries infected with *B. cinerea* at two stages of grapevine development corresponding to berries at veraison stage and ripe berries, respectively. For each bar plot, bars represent the mean ± SEM on three biologically independent experiments and statistically significant groups are categorized by different letters (Kruskal-Wallis/BH post-test; $P<0.05$). All transcriptomic data were generated from Kelloniemi et al. (2015).

**Fig. 2.** *VvLYK6* belongs to the LYRI B phylogenetic clade of the LysM receptor-like kinases family. **(A)** A 1000 bootstrapped Maximum-likelihood phylogenetic tree (Jones-Taylor-Thornton (JTT) model) with LysM-RLKs from 8 plant species was constructed with MEGA X (Kumar *et al.*, 2018). Phylogenetic tree was subdivided by clades according to the phylogenetic analysis from Buendia *et al.* (2018). LYKs correspond to LysM-RLKs with an active kinase domain and LYRs correspond to LYK-related LysM-RLKs without kinase activity.

Protein sequences are listed in supplemental Table S1. The 16 LysM-RLKs found in grapevine genome (VvLYKs) are in bold. VvLYK6 is highlighted in green and indicated by a black arrow inside the green-surrounded LYRI B clade. **(B)** Schematic representation of putative VvLYK6 domains. Black square: Signal peptide, hexagon: LysM domain, LysM1 (orange), LysM2 (blue), LysM3 (green), grey circle: transmembrane domain and blue square: kinase domain. Below schematic VvLYK6 structure are shown alignments of motifs involved in kinase activity (Glycine rich-loop, Catalytic loop (RD) and activation segment (DFG motif). Protein domain sequences were aligned with Clustal performed on MEGAX (Kumar *et al.*, 2018). Black and grey shading representing conservation of amino acids. The alignment includes VvLYK1-1, VvLYK1-2, AtCERK1 belonging to the LYKI clade and MtLYR8, PpLYR2, VvLYK6, SlLYK9, MaLYK7, MaLYK6, OsLysM-RLK11/OsLYR8 and HvRLK2 belonging to the LYRI B clade. **(C)** Subcellular localization of VvLYK6 in *A. thaliana* leaves. GFP-tagged VvLYK6 in leaf segments of *A. thaliana* co-localizes with the plasma membrane marker probe (FM4-64). Plasmolysis of plant cells expressing VvLYK6 tagged with GFP reveals that the GFP signal does not localize to the cell wall. Scale bars represent 20 µm. Similar localization was observed in three independent lines. BF = Brightfield.

**Fig. 3.** Constitutive expression of *VvLYK6* in *A. thaliana* increases its susceptibility to different fungal pathogens. **(A)** Disease lesions percentage induced by *B. cinerea* on Wild-type (WT) and the three independent transgenic lines expressing *VvLYK6* measured 3 days post inoculation, lesion area on WT plants are referred as 100%. Violin plot with included boxplot illustrates the distribution of lesions percentage of three independent experiments. For each biological replicate, 32 lesions were scored from 8 plants per line, combining data from 3 biological replicates. Each transgenic line was statistically compared to the WT with the non-parametric Wilcoxon test (***, $P<0.001$). **(B)** Lesions percentage provoked by the necrotrophic fungus *A. brassicicola* on the WT and the three independent transgenic lines constitutively expressing *VvLYK6,* measured five days post inoculation. Violin plot with included boxplot represents distribution of lesions percentage of five independent experiments. For each biological replicate, 18 lesions were scored from four plants per line, combining data from 4 biological replicates. Each transgenic line was statistically compared to the WT with the non-

parametric Wilcoxon test (***, P<0.001; **, P<0.01; *, P<0.05). **(C)** Penetration of the non-adapted powdery mildew *E. necator* on the WT and the three independent transgenic lines constitutively expressing *VvLYK6* measured 2 days post inoculation. Bars represent the mean percentage of epidermal penetrated cells from three biologically independent experiments each with more than one hundred germinated conidia counted ± SEM. Each transgenic line was statistically compared to the WT with a pairwise comparison of proportions test (***, P<0.001).

**Fig. 4.** Constitutive expression of VvLYK6 inhibits chitin-triggered immune responses in *A. thaliana*. **(A-B)** MAPKs phosphorylation was detected 10 min or 20 min after $H_2O$ (-) or chitin DP6 treatment (0.05 g/L) by immunoblotting with an antibody α-pERK1/2 in the Wild-Type (WT) and three independent lines constitutively expressing *VvLYK6*. (a) Representative immunoblotting with α-pERK1/2 and homogeneous loading verified by Ponceau red staining. **(B)** Quantification of the MAPKs phosphorylation at 10 min after treatment, detected by ImageQuant. Bars represent the mean ± SEM on 6 biologically independent experiments. Each *VvLYK6*-expressing line treated with chitin DP6 was statistically compared to the WT with the non-parametric Wilcoxon test (*, P<0.05). **(C-D)** Normalized expression level of *AtFRK1* and *AtRBOHD* measured by qPCR 1h after chitin DP6 (0.05 g/L) or $H_2O$ treatment. The expression levels of *AtFRK1* and *AtRBOHD* were normalized to those of two housekeeping genes. Bars represent the mean of relative expression ± SEM of 5 biologically independent experiments. Asterisks indicate a statistically significant difference between each transgenic line and the WT treated with chitin DP6, (non-parametric Wilcoxon test; *, P<0.05; **, P<0.01). **(E)** Representative pictures of callose deposition after chitin DP6 (0.05g/L) or $H_2O$ treatment in WT or the three *VvLYK6*-expressing lines, observed 4 days post-treatment and analyzed by epifluorescence microscopy after aniline blue staining. Callose deposits were quantified with Trainable Weka Segmentation plugin in imageJ. **(F)** Box plot represents distribution of callose deposits percentage on total leaves surface for each genotype and condition on at least 30 pictures per condition from three biologically independent experiments. Asterisks indicate a significant difference between each line expressing *VvLYK6* and WT treated with DP6 (Wilcoxon test, ***; P<0.001).

**Fig. 5.** VvLYK6 is also a repressor of chitin-triggered immune responses in *V. vinifera*. **(A)** Quantification of the MAPKs phosphorylation detected 10 min after $H_2O$ or DP6 treatment (0.05 g/L) by immunoblotting with an antibody α-pERK1/2 in the WT grapevine cell line and two independent lines constitutively expressing VvLYK6-GFP. MAPKs phosphorylation was quantified by ImageQuant. Bars represent the mean ± SEM on five biologically independent experiments. Each *VvLYK6*-expressing cell line was statistically compared to the corresponding WT grapevine cells

treated with DP6 using the non-parametric Wilcoxon test (*, P<0.05; **, P <0.01). **(B-C)** Normalized expression level of *VvPAL* **(B)** and V*vSTS1.2* **(C)** measured by qPCR 1h after DP6 (0.05 g/L) or $H_2O$ treatment. The expression levels of *VvPAL and VvSTS1.2* were normalized to those of two housekeeping genes. Bars represent the mean of relative expression ± SEM of 6 biologically independent experiments. Asterisks indicate a statistically significant difference between each transgenic line and the WT treated with DP6 using a pairwise Wilcoxon test (*, P<0.05; **, P <0.01).

**Fig. 6.** VvLYK6 interacts with VvLYK1-1 in presence of chitin oligomers. **(A)** The dead kinase VvLYK1-1$^{G328E}$-CFP was transiently expressed in *Nicotiana benthamiana* leaves alone or together with VvLYK6-YFP or VvLYK5-1-YFP, a protein known to interacts with VvLYK1-1 in presence of chitin DP6 (Roudaire *et al.*, 2023). CFP lifetime (ns) was measured after leaves treatment with either water ($H_2O$) or chitin DP6 (0,1 g/L). Boxplots represent the distribution of the data acquired in at least three biologically independent experiments. Different letters indicate a significant difference using a non-parametric Kruskal-Wallis test. **(B)** Co-immunopurification (Co-IP) of VvLYK1-1$^{G328E}$-HA with VvLYK5-1:YFP and VvLYK6:YFP in presence or not of chitin DP6. Extracted proteins from *N. benthamiana* leaves were purified using anti-HA beads (Anti-HA IP). After IP, corresponding proteins were detected with anti-GFP antibodies (αGFP) and anti-HA antibodies (αHA). **(C)** The LysM-RLK VvLYK6 alone is not able to bind CO5 or CO7 with high affinity. VvLYK6-YFP and BdLYR2-YFP were transiently expressed in *N. benthamiana* leaves. Subsequently, microsomal fractions were prepared, and binding assays were conducted using a range of CO5-biotin or CO7-biotin as ligand. Microsomal fractions from leaves expressing BdLYR2-YFP were used as positive control (black arrow) while those from non-transformed (NT) leaves served as negative control. Western blotting was conducted using αGFP and streptavidin-HRP. The quantities of microsomal fractions used correspond to 50 µg of total proteins for VvLYK6-YFP and NT, and 5 µg for BdLYR2-YFP. The asterisk represents an unspecific band (endogenously biotinylated protein) observed at 130 KDa. No binding with CO5-biotin or CO7-biotin were observed with VvLYK6.

**Fig. 7.** Resveratrol-related pathway is affected in *Vvlyk6* mutants. **(A)** Schematic representation of the *VvLYK6* gene structure highlighting the position of 3 sgRNAs. Alignment of sgRNAs sequence of WT-like and two mutant lines named *Vvlyk6-KO#1* and *Vvlyk6-KO#2.* WT-like non-edited sequence is highlighted in grey and all insertions or deletions are highlighted in red. Two alleles are represented for each mutant to indicate monoallelic and biallelic mutations. **(B)** Illustration of translated proteins in the WT-like and the two mutant lines. Different domain characterizing the LysM-RLK VvLYK6 are represented. Black square: Signal peptide, hexagon: LysM domain, LysM1 (orange), LysM2

(blue), LysM3 (green), grey circle: transmembrane domain and blue square: kinase domain. **(C)** Normalized expression level of *VvSTS1.2* measured by qPCR at basal state in WT-like and KO-*Vvlyk6* mutant lines. The expression levels of *VvSTS1.2* were normalized to those of two housekeeping genes. Bars represent the mean of relative expression ± SEM of 6 biologically independent experiments. Asterisks indicate a statistically significant difference between each mutant *Vvlyk6-KO#1* and *Vvlyk6-KO#2* and WT-like using a non-parametric Wilcoxon test (*, P<0,05; **, P<0,01). **(D)** Amounts of resveratrol semi-quantified by liquid chromatography-mass spectrometry at basal state in WT-like and KO-*Vvlyk6* mutant lines. Bars represent the mean of relative expression ± SEM of 4 biologically independent experiments. Asterisks indicate a statistically significant difference between each mutant and WT-like using non-parametric Wilcoxon test (**, P<0,01; ***, P<0,001).

**Fig. 8.** Proposed mode of action of VvLYK6 to modulate plant immune responses. VvLYK6 is involved in grapevine susceptibility during *Botrytis cinerea* infection and repression of chitin oligomer elicitation. **A)** *VvLYK6* expression is induced during *B. cinerea* infection in mature berries (MB), correlated with the absence of defense gene (*VvSTS1.2* and *VvPAL*) and a high susceptibility to fungal pathogens (Kelloniemi *et al.*, 2015). **B)** Formation of a VvLYK1-1 / VvLYK5-1 complex after perception of chitin oligomers at the plasma membrane to activate a strong MAMP-triggered immunity (MTI) in grapevine cells (Roudaire *et al.*, 2023). **C)** Constitutive expression of VvLYK6, which interacts with VvLYK1-1, might deplete VvLYK1-1 for its interaction with VvLYK5-1 and decrease chitin-triggered plant defense responses. Receptors have been classified by colour, VvLYK1-1 = blue, VvLYK5-1 = red, VvLYK6 = green.

SUPPLEMENTAL INFORMATION

Supplemental figures. Figures S1-S12

Supplemental tables. Tables S1-S3

REFERENCES


**Adrian M, Corio-Costet M-F, Calonnec A, Cluzet S, Poinssot B, Trouvelot S, Wiedemann-Merdinoglu S, Viaud M** (2024) Chapter Four - Grapevine defence mechanisms when challenged by pathogenic fungi and oomycetes. In: Martins-Lopes P, ed. Advances in Botanical Research. Grapevine: From Origin to the Vineyard. Academic Press, 101–195.

**Ahuja I, Kissen R, Bones AM** (2012) Phytoalexins in defense against pathogens. Trends in Plant Science **17**: 73–90

**Ao Y, Li Z, Feng D, Xiong F, Liu J, Li J, Wang M, Wang J, Liu B, Wang H** (2014) OsCERK 1 and OsRLCK 176 play important roles in peptidoglycan and chitin signaling in rice innate immunity. The Plant Journal **80**: 1072–1084

**Böhm H, Albert I, Oome S, Raaymakers TM, Van Den Ackerveken G, Nürnberger T** (2014) A conserved peptide pattern from a widespread microbial virulence factor triggers pattern-induced immunity in Arabidopsis. PLoS Pathog **10**: e1004491

**Boller T, Felix G** (2009) A renaissance of elicitors: Perception of microbe-associated molecular patterns and danger signals by pattern-recognition receptors. Annu Rev Plant Biol **60**: 379–406

**Brandizzi F, Irons SL, Johansen J, Kotzer A, Neumann U** (2004) GFP is the way to glow: bioimaging of the plant endomembrane system. Journal of Microscopy **214**: 138–158

**Brulé D, Villano C, Davies LJ, Trdá L, Claverie J, Héloir M, Chiltz A, Adrian M, Darblade B, Tornero P, et al** (2019) The grapevine (*Vitis vinifera*) LysM receptor kinases Vv LYK 1-1 and Vv LYK 1-2 mediate chitooligosaccharide-triggered immunity. Plant Biotechnology Journal **17**: 812–825

**Buendia L, Wang T, Girardin A, Lefebvre B** (2016) The LysM receptor-like kinase SlLYK10 regulates the arbuscular mycorrhizal symbiosis in tomato. New Phytologist **210**: 184–195

**Buendia L, Girardin A, Wang T, Cottret L, Lefebvre B** (2018) LysM Receptor-Like Kinase and LysM Receptor-Like Protein families: An update on phylogeny and functional characterization. Front Plant Sci **9**: 1531

**Cao Y, Liang Y, Tanaka K, Nguyen CT, Jedrzejczak RP, Joachimiak A, Stacey G** (2014) The kinase LYK5 is a major chitin receptor in Arabidopsis and forms a chitin-induced complex with related kinase CERK1. eLife **3**: e03766

**Claverie J, Balacey S, Lemaître-Guillier C, Brulé D, Chiltz A, Granet L, Noirot E, Daire X, Darblade B, Héloir M-C, et al** (2018) The cell wall-derived xyloglucan is a new DAMP triggering plant immunity in *Vitis vinifera* and *Arabidopsis thaliana*. Front Plant Sci **9**: 1725

**Clough SJ, Bent AF** (1998) Floral dip: a simplified method for *Agrobacterium*-mediated transformation of *Arabidopsis thaliana*. The Plant Journal **16**: 735–743

**Cullimore J, Fliegmann J, Gasciolli V, Gibelin-Viala C, Carles N, Luu T-B, Girardin A, Cumener M, Maillet F, Pradeau S, et al.** (2023) Evolution of lipochitooligosaccharide binding to a LysM-RLK for nodulation in *Medicago truncatula*. Plant And Cell Physiology **64**: 746–757.

**Ding Y, Wang T, Gasciolli V, Reyt G, Remblière C, Marcel F, François T, Bendahmane A, He G, Bono JJ, et al** (2024a) The LysM Receptor-Like Kinase SlLYK10 controls lipochitooligosaccharide signaling in inner cell layers of tomato roots. Plant and Cell Physiology **65**: 1149–1159

**Ding Y, Gasciolli V, Medioni L, Gaston M, de-Regibus A, Rem-blière C, Bono JJ, Cullimore J, Dalmais M, Saffray C, et al** (2024b) A new group of LysM-RLKs involved in symbiotic signal perception and arbuscular mycorrhiza establishment. BioRxiv doi: 10.1101/2024.03.06.583654

**Feechan A, Anderson C, Torregrosa L, Jermakow A, Mestre P, Wiedemann-Merdinoglu S, Merdinoglu D, Walker AR, Cadle-Davidson L, Reisch B, et al** (2013) Genetic dissection of a TIR-NB-LRR locus from the wild North American grapevine species *Muscadinia rotundifolia* identifies paralogous genes conferring resistance to major fungal and oomycete pathogens in cultivated grapevine. The Plant Journal **76**: 661–674

**Feng F, Sun J, Radhakrishnan GV, Lee T, Bozsóki Z, Fort S, Gavrin A, Gysel K, Thygesen MB, Andersen KR, et al** (2019) A combination of chitooligosaccharide and lipochitooligosaccharide recognition promotes arbuscular mycorrhizal associations in Medicago truncatula. Nat Commun **10**: 5047

**Fillinger S, Elad Y, eds** (2016) Botrytis – the Fungus, the Pathogen and its Management in Agricultural Systems. doi: 10.1007/978-3-319-23371-0

**Gabler FM, Smilanick JL, Mansour M, Ramming DW, Mackey BE** (2003) Correlations of morphological, anatomical, and chemical features of grape berries with resistance to *Botrytis cinerea*. Phytopathology® **93**: 1263–1273

**Gamm M, Héloir M-C, Kelloniemi J, Poinssot B, Wendehenne D, Adrian M** (2011) Identification of reference genes suitable for qRT-PCR in grapevine and application for the study of the expression of genes involved in pterostilbene synthesis. Mol Genet Genomics **285**: 273–285

**Gimenez-Ibanez S, Hann DR, Ntoukakis V, Petutschnig E, Lipka V, Rathjen JP** (2009) AvrPtoB targets the LysM Receptor Kinase CERK1 to promote bacterial virulence on plants. Current Biology **19**: 423–429

**Girardin A, Wang T, Ding Y, Keller J, Buendia L, Gaston M, Ribeyre C, Gasciolli V, Auriac M-C, Vernié T, et al** (2019) LCO receptors involved in arbuscular mycorrhiza are functional for rhizobia perception in legumes. Current Biology **29**: 4249-4259.e5

**Haile ZM, Malacarne G, Pilati S, Sonego P, Moretto M, Masuero D, Vrhovsek U, Engelen K, Baraldi E, Moser C** (2020) Dual transcriptome and metabolic analysis of *Vitis vinifera* cv. Pinot Noir berry and *Botrytis cinerea* during quiescence and egressed infection. Front Plant Sci **10**: 1704

**Halter T, Imkampe J, Mazzotta S, Wierzba M, Postel S, Bücherl C, Kiefer C, Stahl M, Chinchilla D, Wang X, et al** (2014) The Leucine-Rich Repeat Receptor Kinase BIR2 is a negative regulator of BAK1 in plant immunity. Current Biology **24**: 134–143

**Hanks SK, Quinn AM, Hunter T** (1988) The protein kinase family: Conserved features and deduced phylogeny of the catalytic domains. Science **241**: 42–52

**Hayafune M, Berisio R, Marchetti R, Silipo A, Kayama M, Desaki Y, Arima S, Squeglia F, Ruggiero A, Tokuyasu K, et al** (2014) Chitin-induced activation of immune signaling by the rice receptor CEBiP relies on a unique sandwich-type dimerization. Proc Natl Acad Sci USA. doi: 10.1073/pnas.1312099111

**He J, Zhang C, Dai H, Liu H, Zhang X, Yang J, Chen X, Zhu Y, Wang D, Qi X, et al** (2019) A LysM receptor heteromer mediates perception of arbuscular mycorrhizal symbiotic signal in rice. Molecular Plant **12**: 1561–1576

**Jones DT, Taylor WR, Thornton JM** (1992) The rapid generation of mutation data matrices from protein sequences. Bioinformatics **8**: 275–282

**Karimi M, De Meyer B, Hilson P** (2005) Modular cloning in plant cells. Trends in Plant Science **10**: 103–105

**Kelloniemi J, Trouvelot S, Héloir M-C, Simon A, Dalmais B, Frettinger P, Cimerman A, Fermaud M, Roudet J, Baulande S, et al** (2015) Analysis of the molecular dialogue between gray mold (*Botrytis cinerea*) and grapevine (*Vitis vinifera*) reveals a clear shift in defense mechanisms during berry ripening. MPMI **28**: 1167–1180

**Klaus-Heisen D, Nurisso A, Pietraszewska-Bogiel A, Mbengue M, Camut S, Timmers T, Pichereaux C, Rossignol M, Gadella TWJ, Imberty A, et al** (2011) Structure-function similarities between a Plant Receptor-like Kinase and the Human Interleukin-1 Receptor-associated Kinase-4. Journal of Biological Chemistry **286**: 11202–11210

**Kumar S, Stecher G, Li M, Knyaz C, Tamura K** (2018) MEGA X: Molecular Evolutionary Genetics Analysis across computing platforms. Molecular Biology and Evolution **35**: 1547–1549

**Li X-R, Sun J, Albinsky D, Zarrabian D, Hull R, Lee T, Jarratt-Barnham E, Chiu CH, Jacobsen A, Soumpourou E, et al** (2022) Nutrient regulation of lipochitooligosaccharide recognition in plants via NSP1 and NSP2. Nat Commun **13**: 6421

**Liu H, Naismith JH** (2008) An efficient one-step site-directed deletion, insertion, single and multiple-site plasmid mutagenesis protocol. BMC Biotechnol **8**: 91

**Liu T, Liu Z, Song C, Hu Y, Han Z, She J, Fan F, Wang J, Jin C, Chang J, et al** (2012) Chitin-induced dimerization activates a plant immune receptor. Science **336**: 1160–1164

**Lovato A, Zenoni S, Tornielli GB, Colombo T, Vandelle E, Polverari A** (2019) Plant and fungus transcriptomic data from grapevine berries undergoing artificially-induced noble rot caused by Botrytis cinerea. Data in Brief **25**: 104150

**Mason KN, Ekanayake G, Heese A** (2020) Staining and automated image quantification of callose in Arabidopsis cotyledons and leaves. Methods in Cell Biology. Elsevier, pp 181–199

**Miya A, Albert P, Shinya T, Desaki Y, Ichimura K, Shirasu K, Narusaka Y, Kawakami N, Kaku H, Shibuya N** (2007) CERK1, a LysM receptor kinase, is essential for chitin elicitor signaling in *Arabidopsis*. Proc Natl Acad Sci USA **104**: 19613–19618

**Morales J, Kadota Y, Zipfel C, Molina A, Torres M-A** (2016) The Arabidopsis NADPH oxidases *RbohD* and *RbohF* display differential expression patterns and contributions during plant immunity. Journal of Experimental Botany **67**: 1663–1676

**Ngou BPM, Heal R, Wyler M, Schmid MW, Jones JDG** (2022) Concerted expansion and contraction of immune receptor gene repertoires in plant genomes. Nat Plants **8**: 1146–1152

**Pathak VM, Verma VK, Rawat BS, Kaur B, Babu N, Sharma A, Dewali S, Yadav M, Kumari R, Singh S, et al** (2022) Current status of pesticide effects on environment, human health and it's eco-friendly management as bioremediation: A comprehensive review. Front Microbiol **13**: 962619

**Puyo M, Scalabrino L, Romanet R, Simonin S, Klein G, Alexandre H, Tourdot-Maréchal R** (2024) Competition for nitrogen resources: An explanation of the effects of a bioprotective strain *Metschnikowia pulcherrima* on the growth of Hanseniaspora Genus in oenology. Foods **13**: 724

**Qiu W, Feechan A, Dry I** (2015) Current understanding of grapevine defense mechanisms against the biotrophic fungus (Erysiphe necator), the causal agent of powdery mildew disease. Hortic Res **2**: 15020

**Roudaire T, Marzari T, Landry D, Löffelhardt B, Gust AA, Jermakow A, Dry I, Winckler P, Héloir M-C, Poinssot B** (2023) The grapevine LysM receptor-like kinase VvLYK5-1 recognizes chitin oligomers through its association with VvLYK1-1. Front Plant Sci **14**: 1130782

**Ruijter JM, Ramakers C, Hoogaars WMH, Karlen Y, Bakker O, Van Den Hoff MJB, Moorman AFM** (2009) Amplification efficiency: linking baseline and bias in the analysis of quantitative PCR data. Nucleic Acids Research **37**: e45–e45

**Schymanski EL, Jeon J, Gulde R, Fenner K, Ruff M, Singer HP, Hollender J** (2014) Identifying small molecules via high resolution mass spectrometry: Communicating confidence. Environ Sci Technol **48**: 2097–2098

**Shimizu T, Nakano T, Takamizawa D, Desaki Y, Ishii-Minami N, Nishizawa Y, Minami E, Okada K, Yamane H, Kaku H, et al** (2010) Two LysM receptor molecules, CEBiP and OsCERK1, cooperatively regulate chitin elicitor signaling in rice: LysM receptors for rice chitin signaling. The Plant Journal **64**: 204–214

**Silva CJ, Van Den Abeele C, Ortega-Salazar I, Papin V, Adaskaveg JA, Wang D, Casteel CL, Seymour GB, Blanco-Ulate B** (2021) Host susceptibility factors render ripe tomato fruit vulnerable to fungal disease despite active immune responses. Journal of Experimental Botany **72**: 2696–2709

**Spoel SH, Koornneef A, Claessens SMC, Korzelius JP, Van Pelt JA, Mueller MJ, Buchala AJ, Métraux J-P, Brown R, Kazan K, et al** (2003) NPR1 modulates cross-talk between Salicylate- and Jasmonate-Dependent defense pathways through a novel function in the cytosol. Plant Cell **15**: 760–770

**Terrier N, Glissant D, Grimplet J, Barrieu F, Abbal P, Couture C, Ageorges A, Atanassova R, Léon C, Renaudin J-P, et al** (2005) Isogene specific oligo arrays reveal multifaceted changes in gene expression during grape berry (*Vitis vinifera* L.) development. Planta **222**: 832–847

**Trdá L, Fernandez O, Boutrot F, Héloir M, Kelloniemi J, Daire X, Adrian M, Clément C, Zipfel C, Dorey S, et al** (2014) The grapevine flagellin receptor VvFLS2 differentially recognizes flagellin-derived epitopes from the endophytic growth-promoting bacterium *Burkholderia*

*phytofirmans* and plant pathogenic bacteria. New Phytologist **201**: 1371–1384

**Vetter MM, Kronholm I, He F, Haweker H, Reymond M, Bergelson J, Robatzek S, De Meaux J** (2012) Flagellin perception varies quantitatively in *Arabidopsis thalia*na and its relatives. Molecular Biology and Evolution **29**: 1655–1667

**Villette J, Lecourieux F, Bastiancig E, Héloir M-C, Poinssot B** (2024) New improvements in grapevine genome editing: high efficiency biallelic homozygous knock-out from regenerated plantlets by using an optimized zCas9i. Plant Methods **20**: 45

**Wan J, Tanaka K, Zhang X-C, Son GH, Brechenmacher L, Nguyen THN, Stacey G** (2012) LYK4, a Lysin Motif Receptor-Like Kinase, is important for chitin signaling and plant innate immunity in Arabidopsis. Plant Physiology **160**: 396–406

**Wang T, Gasciolli V, Gaston M, Medioni L, Cumener M, Buendia L, Yang B, Bono JJ, He G, Lefebvre B** (2023) LysM receptor-like kinases involved in immunity perceive lipo-chitooligosaccharides in mycotrophic plants. Plant Physiology **192**: 1435–1448

**Xiao H, Liu Z, Wang N, Long Q, Cao S, Huang G, Liu W, Peng Y, Riaz S, Walker AM, et al** (2023) Adaptive and maladaptive introgression in grapevine domestication. Proc Natl Acad Sci USA **120**: e2222041120

**Xu L, Wang J, Xiao Y, Han Z, Chai J** (2023) Structural insight into chitin perception by chitin elicitor receptor kinase 1 of *Oryza sativa*. JIPB **65**: 235–248

**Xue D-X, Li C-L, Xie Z-P, Staehelin C** (2019) LYK4 is a component of a tripartite chitin receptor complex in *Arabidopsis thaliana*. Journal of Experimental Botany **70**: 5507–5516

**Zaidi SS-A, Mukhtar MS, Mansoor S** (2018) Genome Editing: Targeting Susceptibility Genes for Plant Disease Resistance. Trends in Biotechnology **36**: 898–906

**Zhang C, He J, Dai H, Wang G, Zhang X, Wang C, Shi J, Chen X, Wang D, Wang E** (2021) Discriminating symbiosis and immunity signals by receptor competition in rice. Proc Natl Acad Sci USA **118**: e2023738118

**Zhou J-M, Zhang Y** (2020) Plant immunity: Danger perception and signaling. Cell **181**: 978–989

**Zimmerli L, Métraux J-P, Mauch-Mani B**. (2001) β-Aminobutyric acid-induced protection of Arabidopsis against the necrotrophic fungus *Botrytis cinerea*. *Plant Physiology* **126**: 517–523.

**Zipfel C** (2014) Plant pattern-recognition receptors. Trends in Immunology **35**: 345–351

**Zouine M, Maza E, Djari A, Lauvernier M, Frasse P, Smouni A, Pirrello J, Bouzayen M**. (2017) TomExpress, a unified tomato RNA-Seq platform for visualization of expression data, clustering and correlation networks. *The Plant Journal* **92**: 727–735.

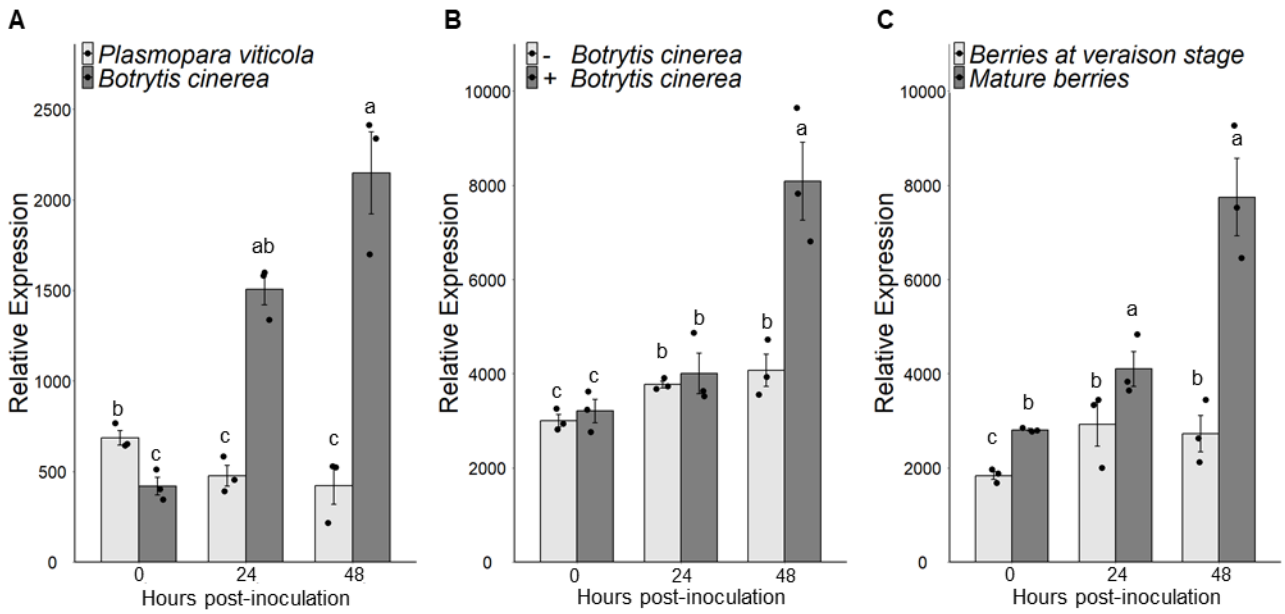


**Fig. 1.** *VvLYK6* is induced during *Botrytis cinerea* infection on grapevine leaves and mature berries. **(A)** *VvLYK6* expression profiles analyzed at 0, 24 and 48 h post-inoculation on leaves infected either by *Botrytis cinerea* or *Plasmopara viticola*. **(B)** *VvLYK6* expression profiles analyzed at 0, 24 and 48 h post-inoculation on ripe berries infected or not with *B. cinerea*. **(C)** Comparison of *VvLYK6* expression on grapevine berries infected with *B. cinerea* at two stages of grapevine development corresponding to berries at veraison stage and ripe berries, respectively. For each bar plot, bars represent the mean ± SEM on three biologically independent experiments and statistically significant groups are categorized by different letters (Kruskal-Wallis/BH post-test; P<0.05). All transcriptomic data were generated from Kelloniemi et al. (2015).

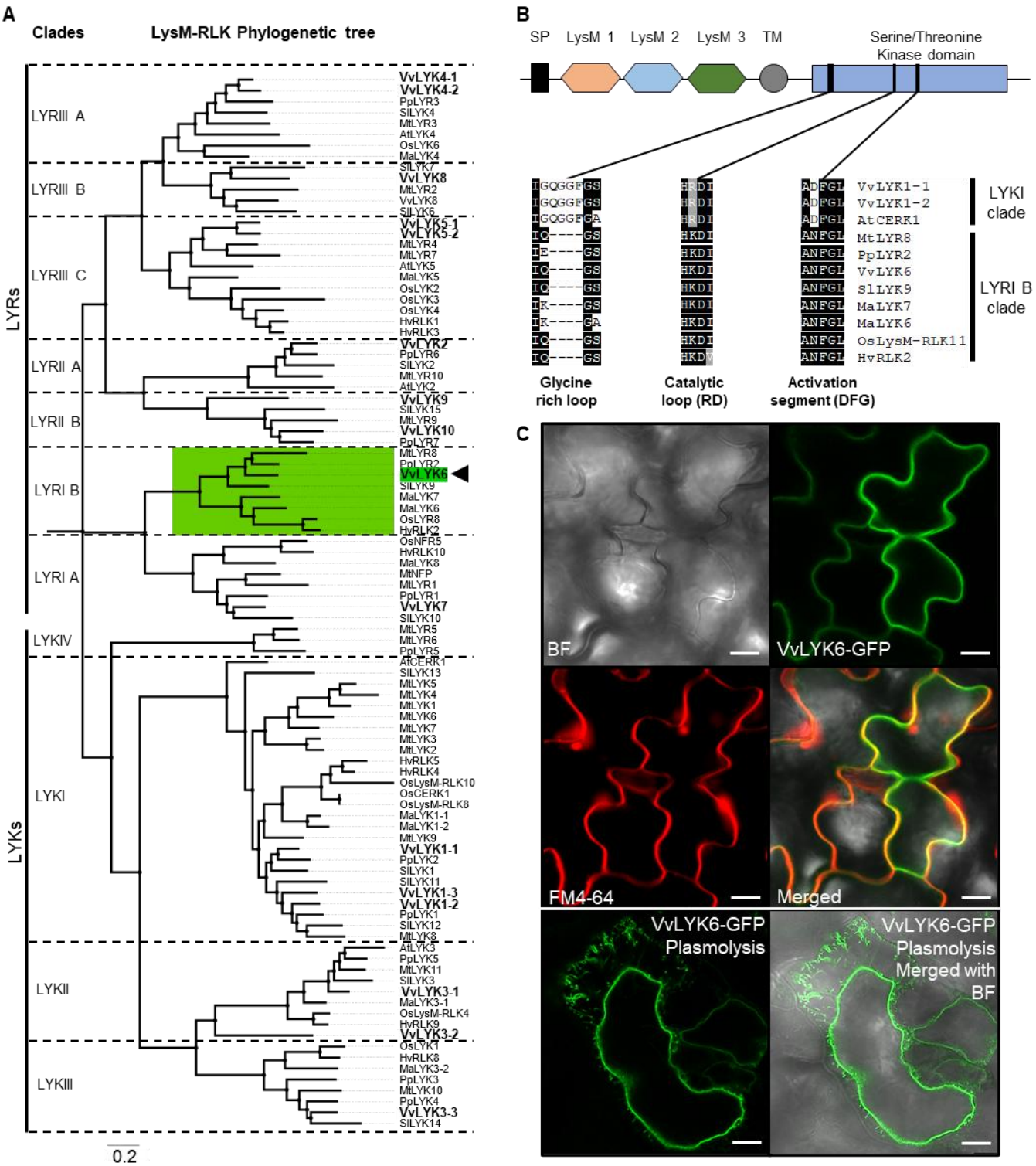


**Fig. 2.** *VvLYK6* belongs to the LYRI B phylogenetic clade of the LysM receptor-like kinases family. **(A)** A 1000 bootstrapped Maximum-likelihood phylogenetic tree (Jones-Taylor-Thornton (JTT) model) with LysM-RLKs from 8 plant species was constructed with MEGA X (Kumar *et al.*, 2018). Phylogenetic tree was subdivided by clades according to the phylogenetic analysis from Buendia *et al.* (2018). LYKs correspond to LysM-RLKs with an active kinase domain and LYRs correspond to LYK-related LysM-RLKs without kinase activity.
Protein sequences are listed in supplemental Table S1. The 16 LysM-RLKs found in grapevine genome (VvLYKs) are in bold. VvLYK6 is highlighted in green and indicated by a black arrow inside the green-surrounded LYRI B clade. **(B)** Schematic representation of putative VvLYK6 domains. Black square: Signal peptide, hexagon: LysM domain, LysM1 (orange), LysM2 (blue), LysM3 (green), grey circle: transmembrane domain and blue square: kinase domain. Below schematic VvLYK6 structure are shown alignments of motifs involved in kinase activity (Glycine rich-loop, Catalytic loop (RD) and activation segment (DFG motif). Protein domain sequences were aligned with Clustal performed on MEGAX (Kumar *et al.*, 2018). Black and grey shading representing conservation of amino acids. The alignment includes VvLYK1-1, VvLYK1-2, AtCERK1 belonging to the LYKI clade and MtLYR8, PpLYR2, VvLYK6, SlLYK9, MaLYK7, MaLYK6, OsLysM-RLK11/OsLYR8 and HvRLK2 belonging to the LYRI B clade. **(C)** Subcellular localization of VvLYK6 in *A. thaliana* leaves. GFP-tagged VvLYK6 in leaf segments of *A. thaliana* co-localizes with the plasma membrane marker probe (FM4-64). Plasmolysis of plant cells expressing VvLYK6 tagged with GFP reveals that the GFP signal does not localize to the cell wall. Scale bars represent 20 µm. Similar localization was observed in three independent lines. BF = Brightfield.



940

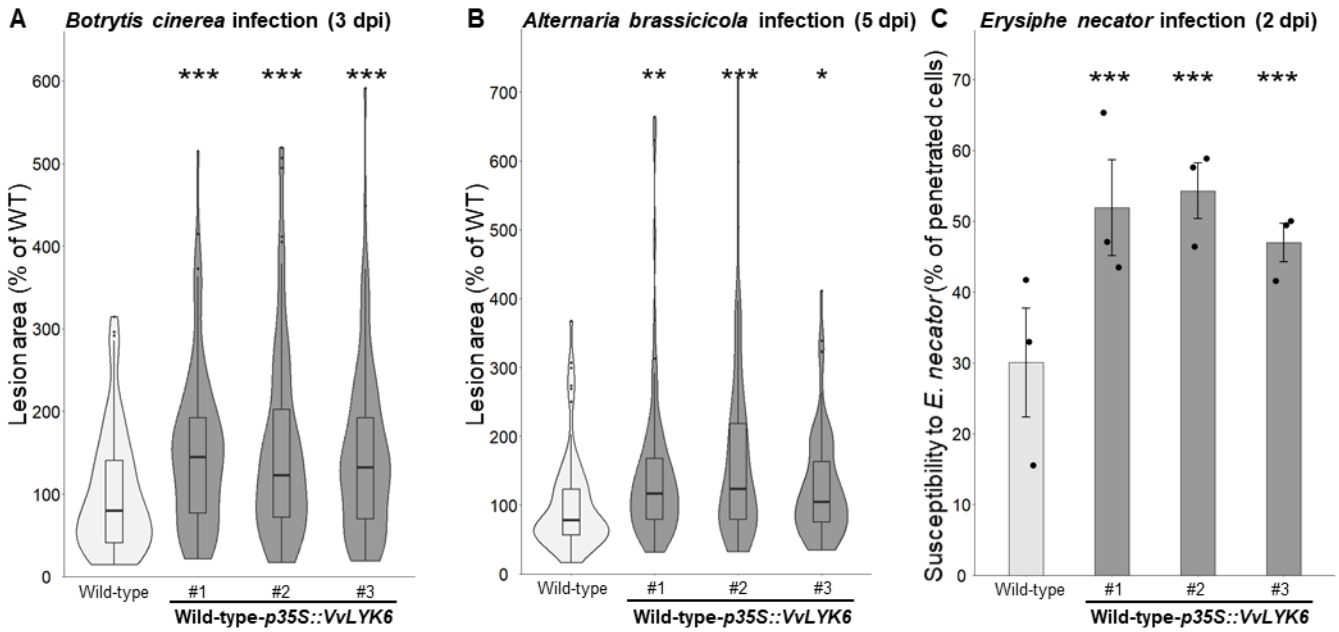


**Fig. 3.** Constitutive expression of *VvLYK6* in *A. thaliana* increases its susceptibility to different fungal pathogens. **(A)** Disease lesions percentage induced by *B. cinerea* on Wild-type (WT) and the three independent transgenic lines expressing *VvLYK6* measured 3 days post inoculation, lesion area on WT plants are referred as 100%. Violin plot with included boxplot illustrates the distribution of lesions percentage of three independent experiments. For each biological replicate, 32 lesions were scored from 8 plants per line, combining data from 3 biological replicates. Each transgenic line was statistically compared to the WT with the non-parametric Wilcoxon test (***, P<0.001). **(B)** Lesions percentage provoked by the necrotrophic fungus *A. brassicicola* on the WT and the three independent transgenic lines constitutively expressing *VvLYK6,* measured five days post inoculation. Violin plot with included boxplot represents distribution of lesions percentage of five independent experiments. For each biological replicate, 18 lesions were scored from four plants per line, combining data from 4 biological replicates. Each transgenic line was statistically compared to the WT with the non-parametric Wilcoxon test (***, P<0.001; **, P<0.01; *, P<0.05). **(C)** Penetration of the non-adapted powdery mildew *E. necator* on the WT and the three independent transgenic lines constitutively expressing *VvLYK6* measured 2 days post inoculation. Bars represent the mean percentage of epidermal penetrated cells from three biologically independent experiments each with more than one hundred germinated conidia counted ± SEM. Each transgenic line was statistically compared to the WT with a pairwise comparison of proportions test (***, P<0.001).

941

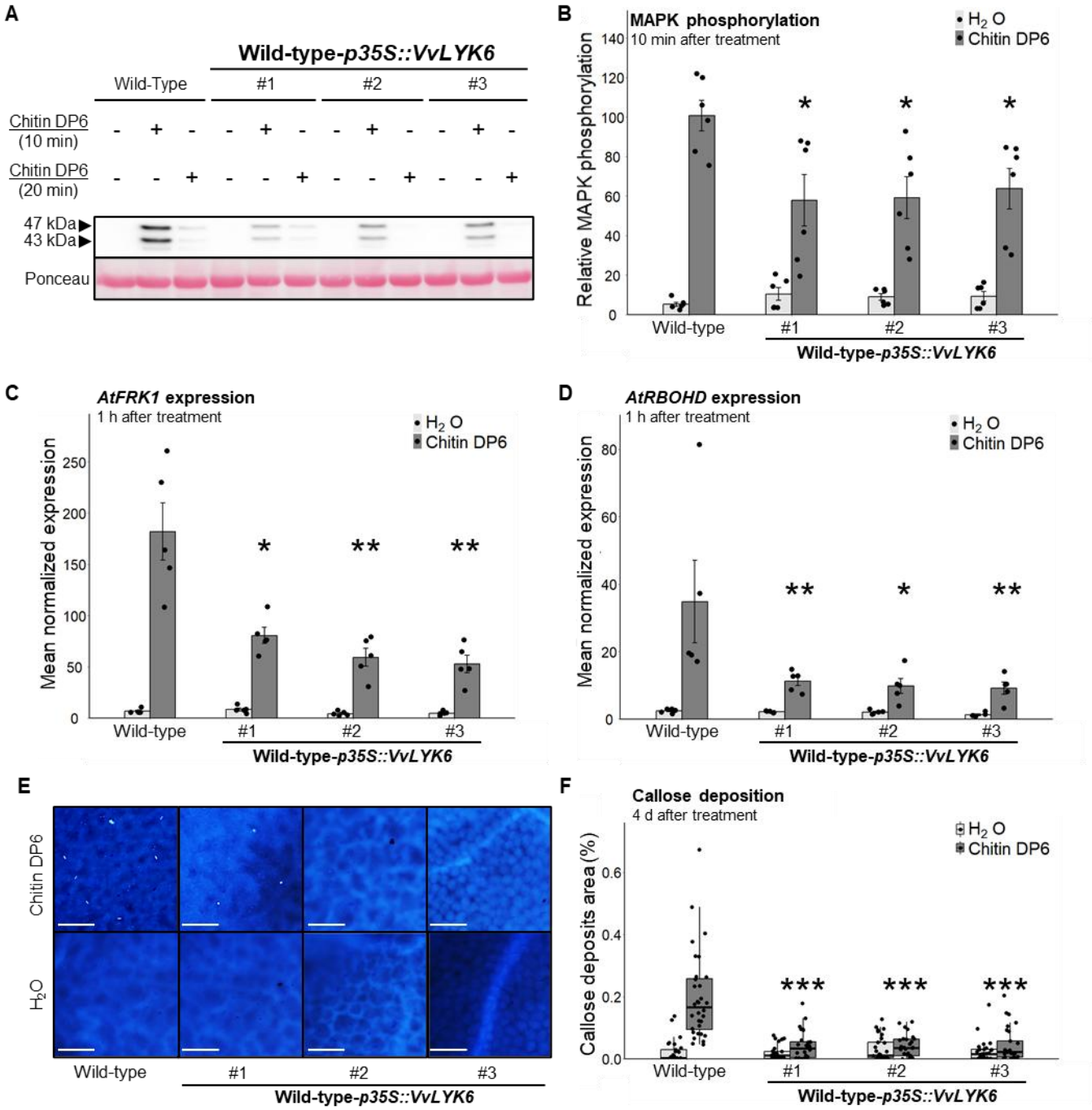


**Fig. 4.** Constitutive expression of VvLYK6 inhibits chitin-triggered immune responses in *A. thaliana*. **(A-B)** MAPKs phosphorylation was detected 10 min or 20 min after $H_2O$ (-) or chitin DP6 treatment (0.05 g/L) by immunoblotting with an antibody α-pERK1/2 in the Wild-Type (WT) and three independent lines constitutively expressing *VvLYK6*. (a) Representative immunoblotting with α-pERK1/2 and homogeneous loading verified by Ponceau red staining. **(B)** Quantification of the MAPKs phosphorylation at 10 min after treatment, detected by ImageQuant. Bars represent the mean ± SEM on 6 biologically independent experiments. Each *VvLYK6*-expressing line treated with chitin DP6 was statistically compared to the WT with the non-parametric Wilcoxon test (*, P<0.05). **(C-D)** Normalized expression level of *AtFRK1* and *AtRBOHD* measured by qPCR 1h after chitin DP6 (0.05 g/L) or $H_2O$ treatment. The expression levels of *AtFRK1* and *AtRBOHD* were normalized to those of two housekeeping genes. Bars represent the mean of relative expression ± SEM of 5 biologically independent experiments. Asterisks indicate a statistically significant difference between each transgenic line and the WT treated with chitin DP6, (non-parametric Wilcoxon test; *, P<0.05; **, P<0.01). **(E)** Representative pictures of callose deposition after chitin DP6 (0.05g/L) or $H_2O$ treatment in WT or the three *VvLYK6*-expressing lines, observed 4 days post-treatment and analyzed by epifluorescence microscopy after aniline blue staining. Callose deposits were quantified with Trainable Weka Segmentation plugin in imageJ. **(F)** Box plot represents distribution of callose deposits percentage on total leaves surface for each genotype and condition on at least 30 pictures per condition from three biologically independent experiments. Asterisks indicate a significant difference between each line expressing *VvLYK6* and WT treated with DP6 (Wilcoxon test, ***; P<0.001).

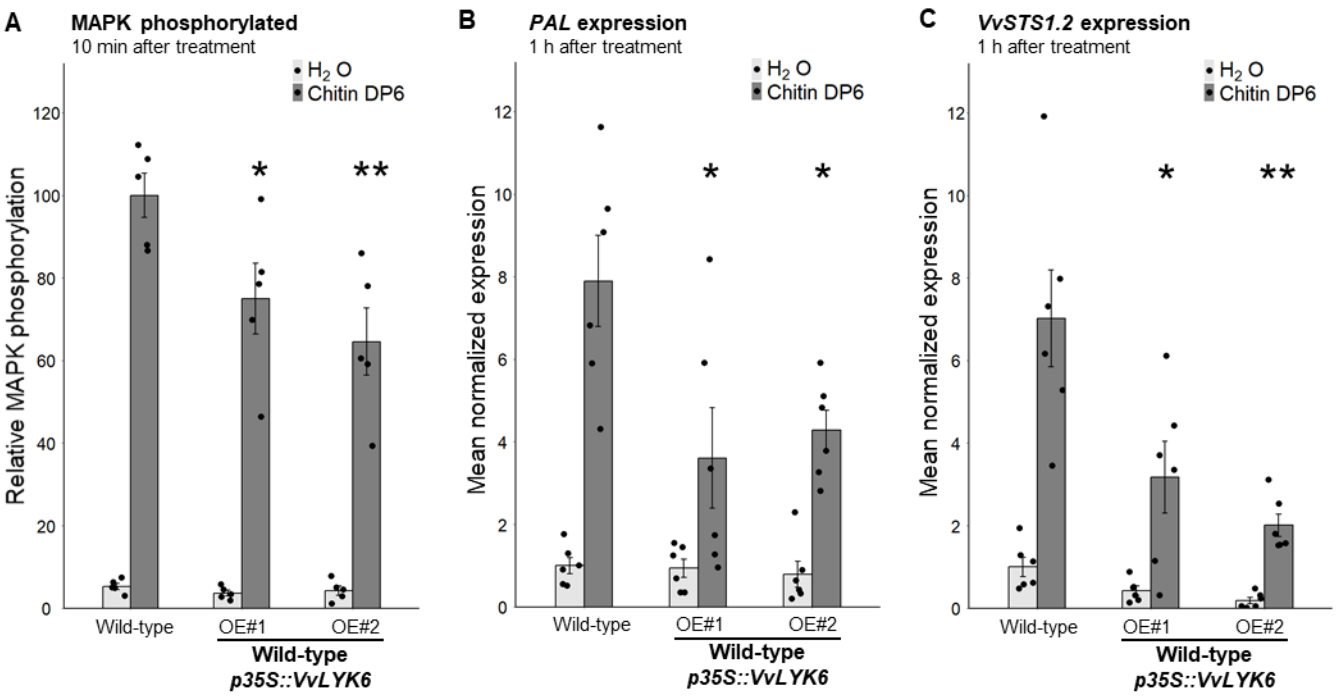


**Fig. 5.** VvLYK6 is also a repressor of chitin-triggered immune responses in *V. vinifera*. **(A)** Quantification of the MAPKs phosphorylation detected 10 min after $H_2O$ or DP6 treatment (0.05 g/L) by immunoblotting with an antibody α-pERK1/2 in the WT grapevine cell line and two independent lines constitutively expressing VvLYK6-GFP. MAPKs phosphorylation was quantified by ImageQuant. Bars represent the mean ± SEM on five biologically independent experiments. Each *VvLYK6*-expressing cell line was statistically compared to the corresponding WT grapevine cells treated with DP6 using the non-parametric Wilcoxon test (*, P<0.05; **, P <0.01). **(B-C)** Normalized expression level of *VvPAL* **(B)** and V*vSTS1.2* **(C)** measured by qPCR 1h after DP6 (0.05 g/L) or $H_2O$ treatment. The expression levels of *VvPAL and VvSTS1.2* were normalized to those of two housekeeping genes. Bars represent the mean of relative expression ± SEM of 6 biologically independent experiments. Asterisks indicate a statistically significant difference between each transgenic line and the WT treated with DP6 using a pairwise Wilcoxon test (*, P<0.05; **, P <0.01).

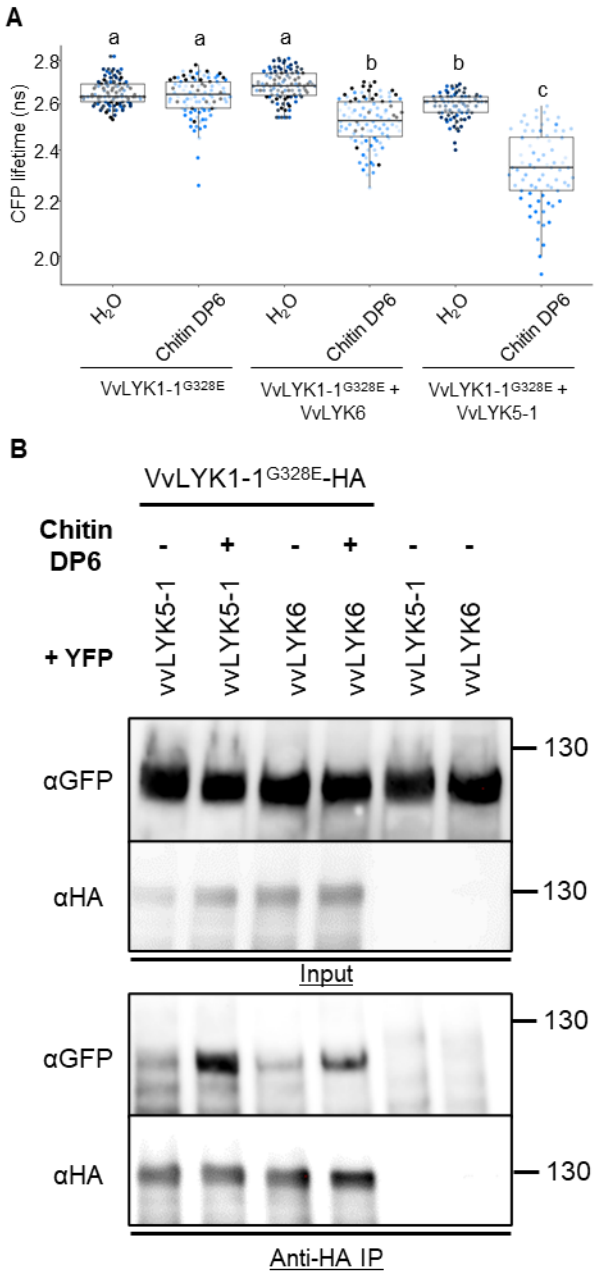


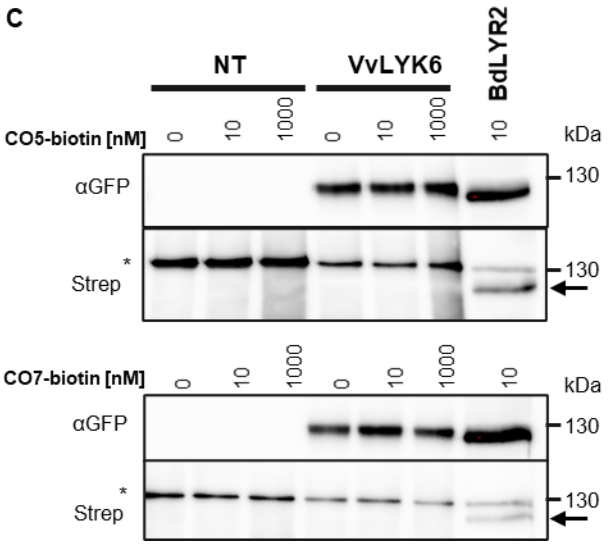


**Fig. 6.** VvLYK6 interacts with VvLYK1-1 in presence of chitin oligomers. **(A)** The dead kinase VvLYK1-1$^{G328E}$-CFP was transiently expressed in *Nicotiana benthamiana* leaves alone or together with VvLYK6-YFP or VvLYK5-1-YFP, a protein known to interacts with VvLYK1-1 in presence of chitin DP6 (Roudaire *et al.*, 2023). CFP lifetime (ns) was measured after leaves treatment with either water ($H_2O$) or chitin DP6 (0,1 g/L). Boxplots represent the distribution of the data acquired in at least three biologically independent experiments. Different letters indicate a significant difference using a non-parametric Kruskal-Wallis test. **(B)** Co-immunopurification (Co-IP) of VvLYK1-1$^{G328E}$-HA with VvLYK5-1:YFP and VvLYK6:YFP in presence or not of chitin DP6. Extracted proteins from *N. benthamiana* leaves were purified using anti-HA beads (Anti-HA IP). After IP, corresponding proteins were detected with anti-GFP antibodies (αGFP) and anti-HA antibodies (αHA). **(C)** The LysM-RLK VvLYK6 alone is not able to bind CO5 or CO7 with high affinity. VvLYK6-YFP and BdLYR2-YFP were transiently expressed in *N. benthamiana* leaves. Subsequently, microsomal fractions were prepared, and binding assays were conducted using a range of CO5-biotin or CO7-biotin as ligand. Microsomal fractions from leaves expressing BdLYR2-YFP were used as positive control (black arrow) while those from non-transformed (NT) leaves served as negative control. Western blotting was conducted using αGFP and streptavidin-HRP. The quantities of microsomal fractions used correspond to 50 µg of total proteins for VvLYK6-YFP and NT, and 5 µg for BdLYR2-YFP. The asterisk represents an unspecific band (endogenously biotinylated protein) observed at 130 KDa. No binding with CO5-biotin or CO7-biotin were observed with VvLYK6.

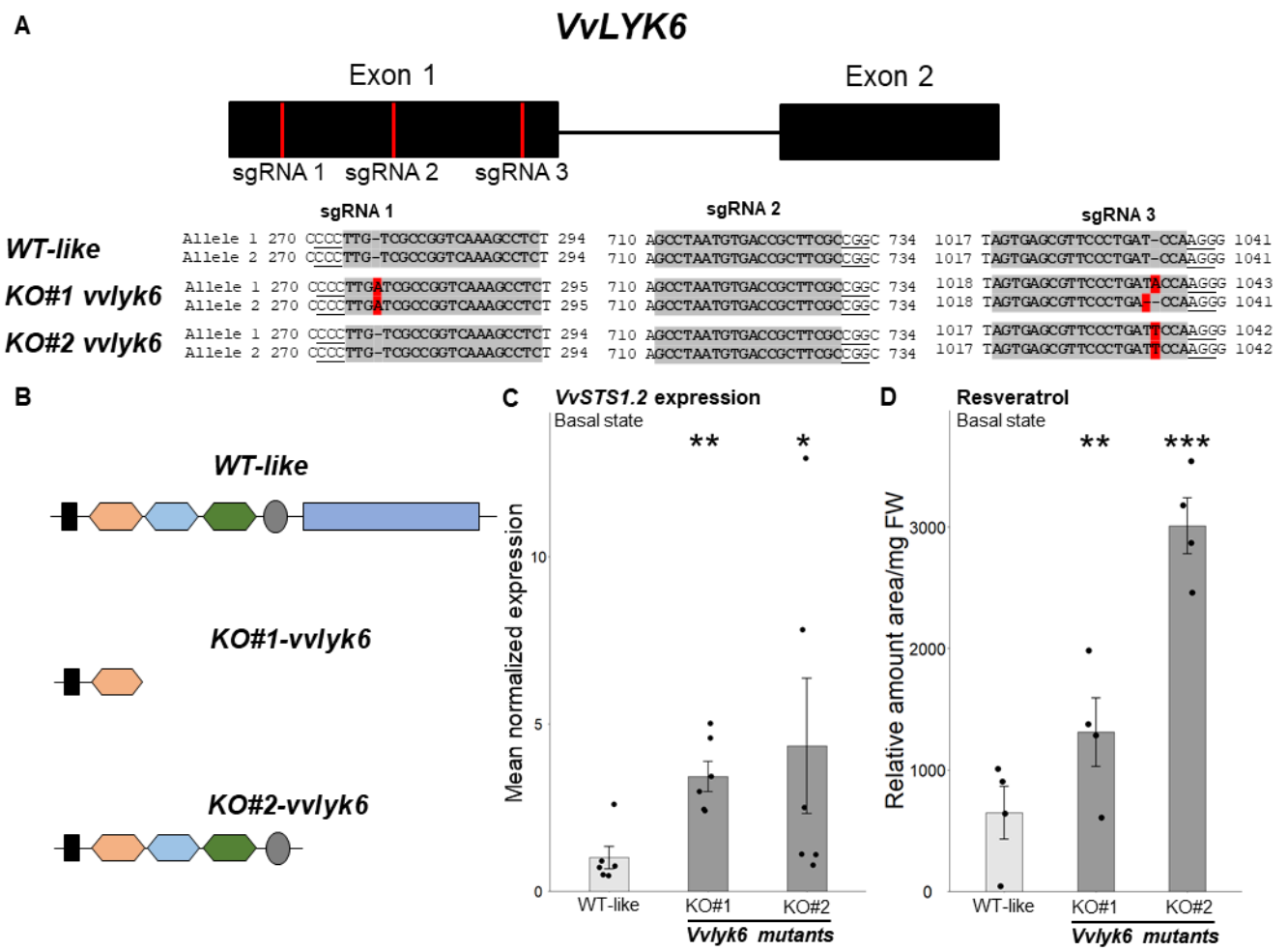


**Fig. 7.** Resveratrol-related pathway is affected in *Vvlyk6* mutants. **(A)** Schematic representation of the *VvLYK6* gene structure highlighting the position of 3 sgRNAs. Alignment of sgRNAs sequence of WT-like and two mutant lines named *Vvlyk6-KO#1* and *Vvlyk6-KO#2*. WT-like non-edited sequence is highlighted in grey and all insertions or deletions are highlighted in red. Two alleles are represented for each mutant to indicate monoallelic and biallelic mutations. **(B)** Illustration of translated proteins in the WT-like and the two mutant lines. Different domain characterizing the LysM-RLK VvLYK6 are represented. Black square: Signal peptide, hexagon: LysM domain, LysM1 (orange), LysM2 (blue), LysM3 (green), grey circle: transmembrane domain and blue square: kinase domain. **(C)** Normalized expression level of *VvSTS1.2* measured by qPCR at basal state in WT-like and KO-*Vvlyk6* mutant lines. The expression levels of *VvSTS1.2* were normalized to those of two housekeeping genes. Bars represent the mean of relative expression ± SEM of 6 biologically independent experiments. Asterisks indicate a statistically significant difference between each mutant *Vvlyk6-KO#1* and *Vvlyk6-KO#2* and WT-like using a non-parametric Wilcoxon test (*, P<0,05; **, P<0,01). **(D)** Amounts of resveratrol semi-quantified by liquid chromatography-mass spectrometry at basal state in WT-like and KO-*Vvlyk6* mutant lines. Bars represent the mean of relative expression ± SEM of 4 biologically independent experiments. Asterisks indicate a statistically significant difference between each mutant and WT-like using non-parametric Wilcoxon test (**, P<0,01; ***, P<0,001).

947

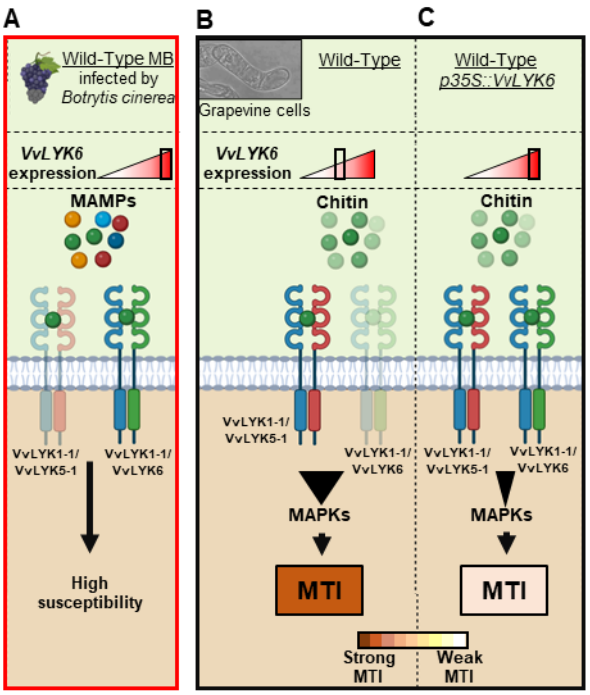


**Fig. 8.** Proposed mode of action of VvLYK6 to modulate plant immune responses. VvLYK6 is involved in grapevine susceptibility during *Botrytis cinerea* infection and repression of chitin oligomer elicitation. **(A)** *VvLYK6* expression is induced during *Botrytis cinerea* infection in mature berries (MB), correlated with the absence of defense gene (*VvSTS1.2* and *VvPAL*) and a high susceptibility to fungal pathogens (Kelloniemi *et al.*, 2015). **(B)** Formation of a VvLYK1-1 / VvLYK5-1 complex after perception of chitin oligomers at the plasma membrane to activate a strong MAMP-triggered immunity (MTI) in grapevine cells (Roudaire *et al.*, 2023). **(C)** Constitutive expression of VvLYK6, which interacts with VvLYK1-1, might deplete VvLYK1-1 for its interaction with VvLYK5-1 and decrease chitin-triggered plant defense responses. Receptors have been classified by colour, VvLYK1-1 = blue, VvLYK5-1 = red, VvLYK6 = green.

948